MODELLING NEUTRINO-NUCLEUS INTERACTIONS FOR OSCILLATION EXPERIMENTS

Maria Barbaro
University of Turin and INFN

TNPI2023
XIX Conference on Theoretical Nuclear Physics in Italy
Cortona, 11-13 OCT 2023

Collaborators

Turin: A. De Pace, **V. Belocchi**
Seville: J.A. Caballero, G.D. Megias, **J.M. Franco-Patiño**, J. Gonzalez-Rosa
Granada: J.E. Amaro, I. Ruiz Simo, P. Casale
Madrid: R. Gonzalez-Jimenez, J.M. Udias
Pavia: C. Giusti
Sofia: A. Antonov, M. Ivanov
MIT: T.W. Donnelly

Motivation: Neutrino Physics

- Neutrinos are building blocks of the Standard Model and powerful tools to explore the Universe.

- Many years after their discovery in 1956, neutrinos are still mysterious particles:

- we know **neutrinos oscillate** but we don't know exactly how

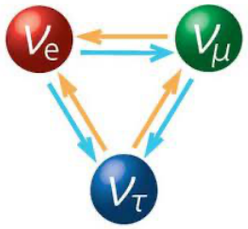

$$P_{\nu_\alpha \to \nu_\beta} = \left| \langle \nu_\alpha | \nu_\beta(t) \rangle \right|^2 = \left| \sum_i U^*_{\alpha i} U_{\beta i} e^{i m_i^2 L/2E_\nu} \right|^2$$

PMNS matrix U encodes oscillation parameters

- are they **Dirac or Majorana**?

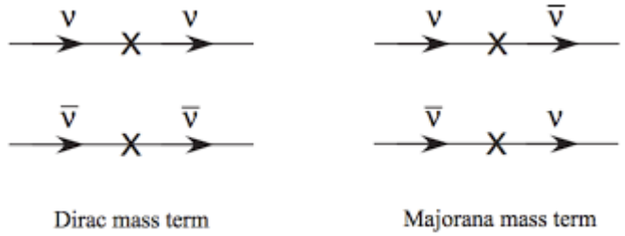

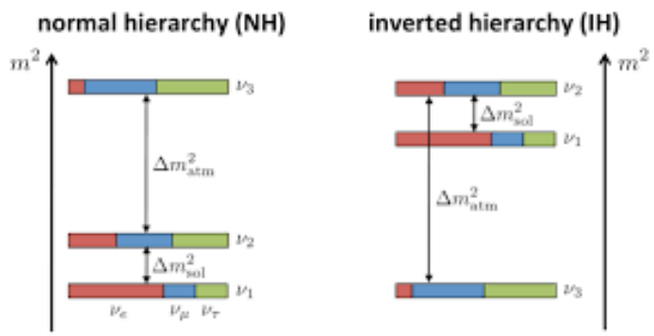

- what are their **masses** and how are they ordered?

- are there **more than three families** of neutrinos (sterile ν)?

- Differences between ν and $\bar{\nu}$ interactions would signal **violation of CP symmetry in the leptonic sector** which would explain part of the **matter/antimatter asymmetry** in the Universe.

Recent constraints from T2K experiment

$$\delta_{CP} = \begin{cases} -1.89\ (+0.70, -0.58) & \text{NH} \\ -1.38\ (+0.48, -0.54) & \text{IH} \end{cases}$$

T2K coll., Nature 580 (2020)

first indication of CP violation in the lepton sector

The precision era for neutrino oscillation

- An intense experimental program aims at answering these fundamental questions with high precision measurements.
- In particular, in **long-baseline oscillation experiments** neutrinos with ~ GeV energy travel between two detectors situated at ~100s Km distance. The appearance or disappearance of neutrinos of given flavour provides information on oscillation parameters.
- Cross sections are extremely small ~10^{-38} cm^2: intense beams and large detectors made of medium/heavy nuclei are needed. Experimental analyses **need nuclear physics input.**

Goals

- leptonic CP violation matter/antimatter asymmetry
- ν masses and hierarchy
- precise oscillation angles
- Dirac or Majorana ν
- sterile neutrinos?

Detectors: Carbon, Oxygen, Argon

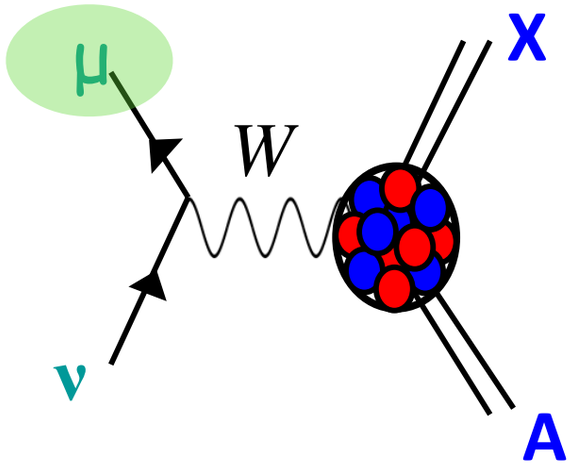

Charged Current
CC

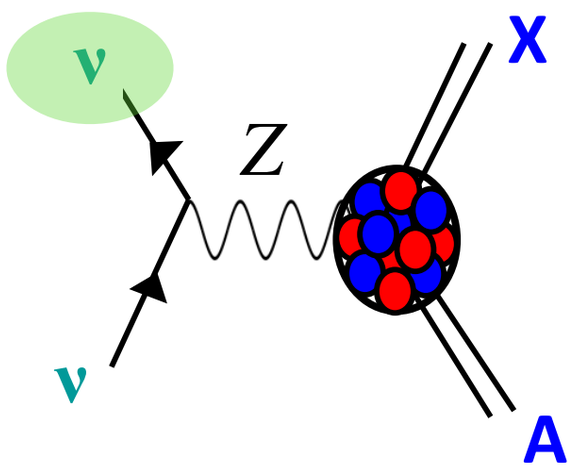

Neutral Current
NC

Long baseline oscillations experiments

J-PARC

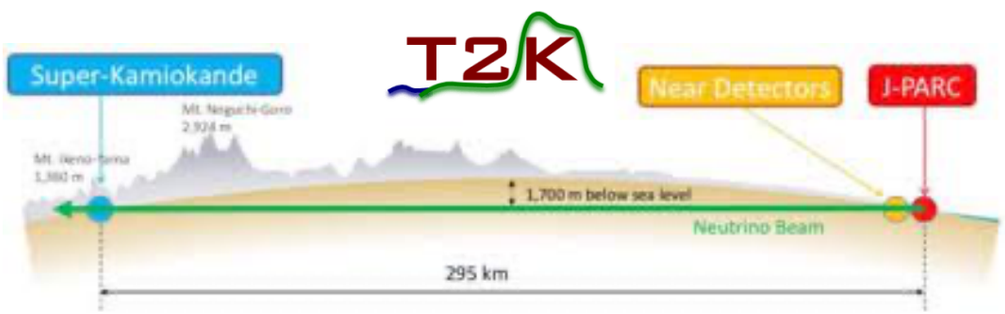

Fermi Lab

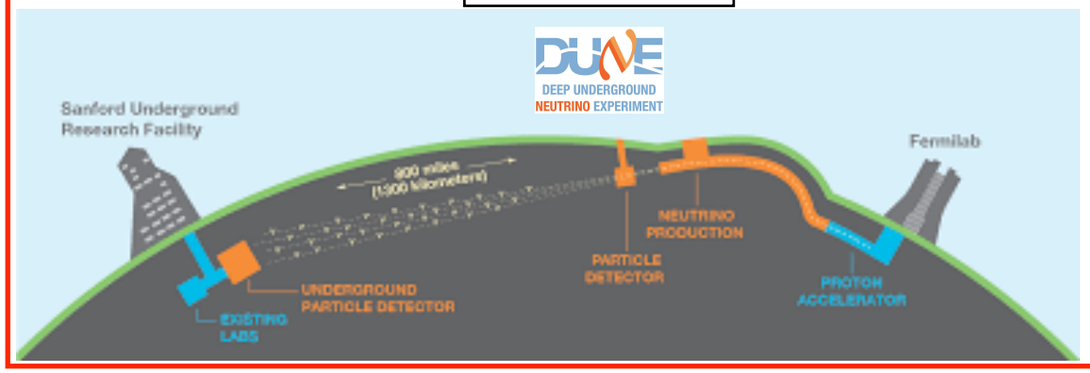

Running **T2K**

Future **HyperK**

Running **NOvA**

Future **DUNE**

Other experiments collecting cross section data

MicroBooNE
largest LArTPC detector

MINERvA
dedicated to $\sigma_{\nu A}$ on different nuclei

Systematic uncertainties

Source (T2K)	$N(\nu_e)$
$\sigma_{\nu N}$ and FSI	3.8%
Total Syst.	**5.2%**

NEUTRINO 2022
XXX International Conference on Neutrino Physics and Astrophysics

Source (NOvA)	$N(\nu_e)$
$\sigma_{\nu N}$ and FSI	7.7%
Total Syst.	**9.2%**

Phys. Rev. D **98**, 032012

Neutrino interaction uncertainties dominate the systematic error They must be reduced for DUNE and HYPERK to succeed

The problem of flux-integration

- **the neutrino energy E_ν is unknown**:
  broad flux distribution, ν beams are non monochromatic

- the neutrino energy is reconstructed from the detected final state using event generators: **nuclear model dependence**

What experimentalists would like to measure

Neutrino flux

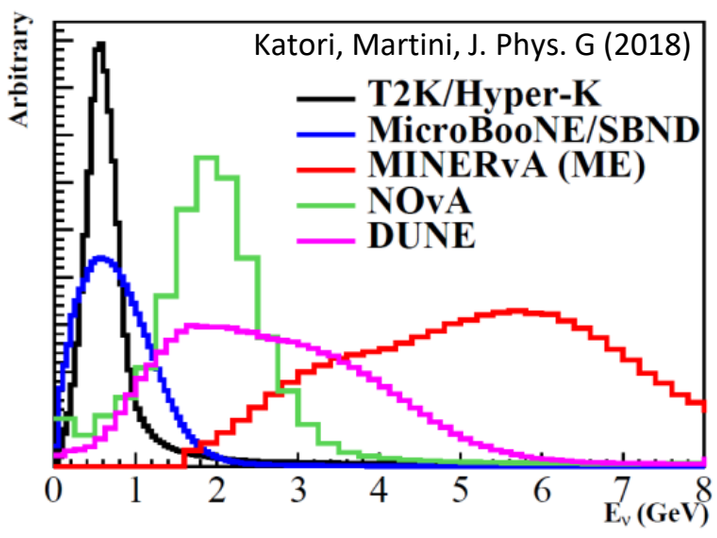

Oscillation probability from flavour α to β

$$P_{\nu_\alpha \to \nu_\beta} = \left| \langle \nu_\alpha | \nu_\beta(t) \rangle \right|^2 = \left| \sum_i U^*_{\alpha i} U_{\beta i} e^{i m_i^2 L/2E_\nu} \right|^2$$

What they do measure

Number of detected events: convolution over the true neutrino energy spectrum

$$N_{\nu_\beta}(\overline{E}_\nu) \sim \int \Phi_{\nu_\alpha}(E_\nu) \times P_{\nu_\alpha \to \nu_\beta}(E_\nu, L, \{\theta\}) \times \sigma_{\nu_\beta}(E_\nu) \times \epsilon_{\text{det.}} \times d(E_\nu, \overline{E}_\nu)\, dE_\nu$$

- $N_{\nu_\beta}(\overline{E}_\nu)$: reconstructed ν energy
- $\Phi_{\nu_\alpha}(E_\nu)$: ν flux
- $P_{\nu_\alpha \to \nu_\beta}(E_\nu, L, \{\theta\})$: oscillation probability
- $\sigma_{\nu_\beta}(E_\nu)$: $\nu - A$ cross section
- $\epsilon_{\text{det.}}$: detector efficiency
- $d(E_\nu, \overline{E}_\nu)$: migration matrix
- dE_ν: true ν energy

Nuclear processes

$$\nu_\mu + A \rightarrow \mu^- + X$$

$$\left\langle \frac{d\sigma}{dk_\mu d\Omega_\mu} \right\rangle = \int dE_\nu \, \Phi(E_\nu) \left[\frac{d\sigma}{dk_\mu d\Omega_\mu} \right]_{E_\nu}$$

flux-averaged cross section

Due to the flux integration different processes contribute to the same experimental signal and cannot be separated

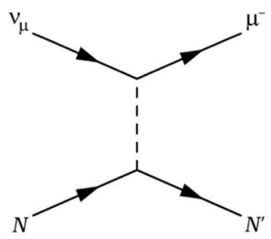

QE
elastic interaction with a bound nucleon

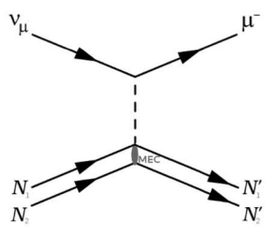

2p2h
interaction with a pair of correlated nucleons
Meson Exchange Currents

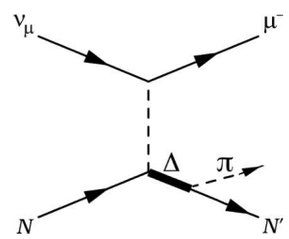

RES
resonance production

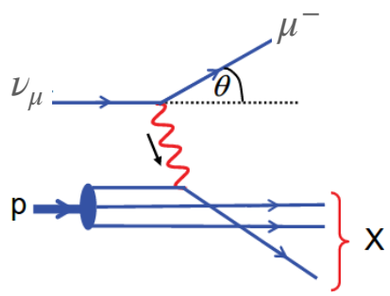

DIS
deep inelastic scattering interaction with quarks

Nuclear models are implemented in Monte Carlo generators (GENIE, NEUT, NUWRO, GIBUU)

- In principle a generator should contain consistent models valid across the full spectrum.
- In practice tunings to specific data are performed, often hiding the correct physics.

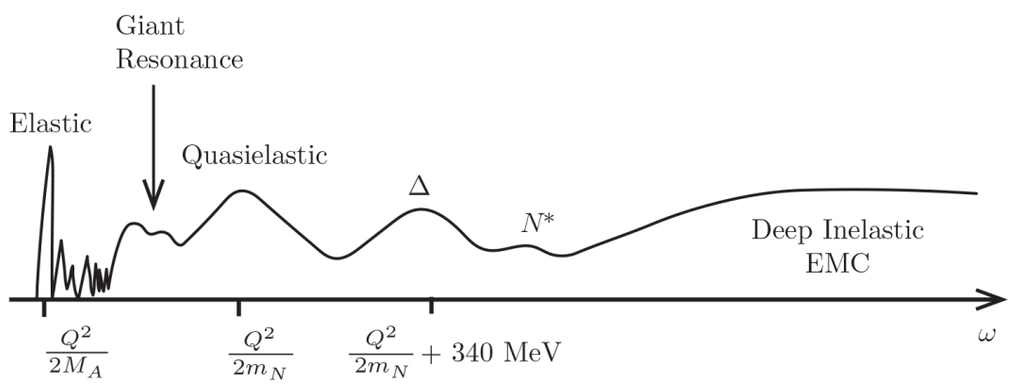

A prominent example: the "M_A puzzle"

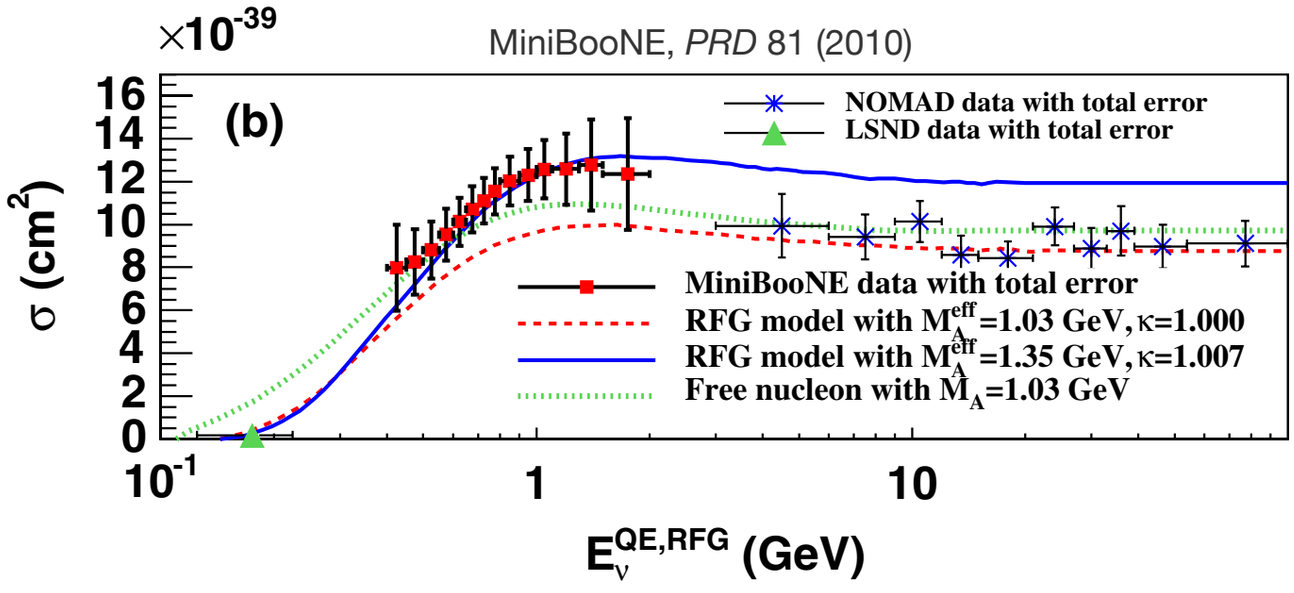

The MiniBooNE neutrino-carbon data analysed using the relativistic Fermi gas model asked for an axial mass M_A=1.35 GeV larger than the standard value of 1 GeV

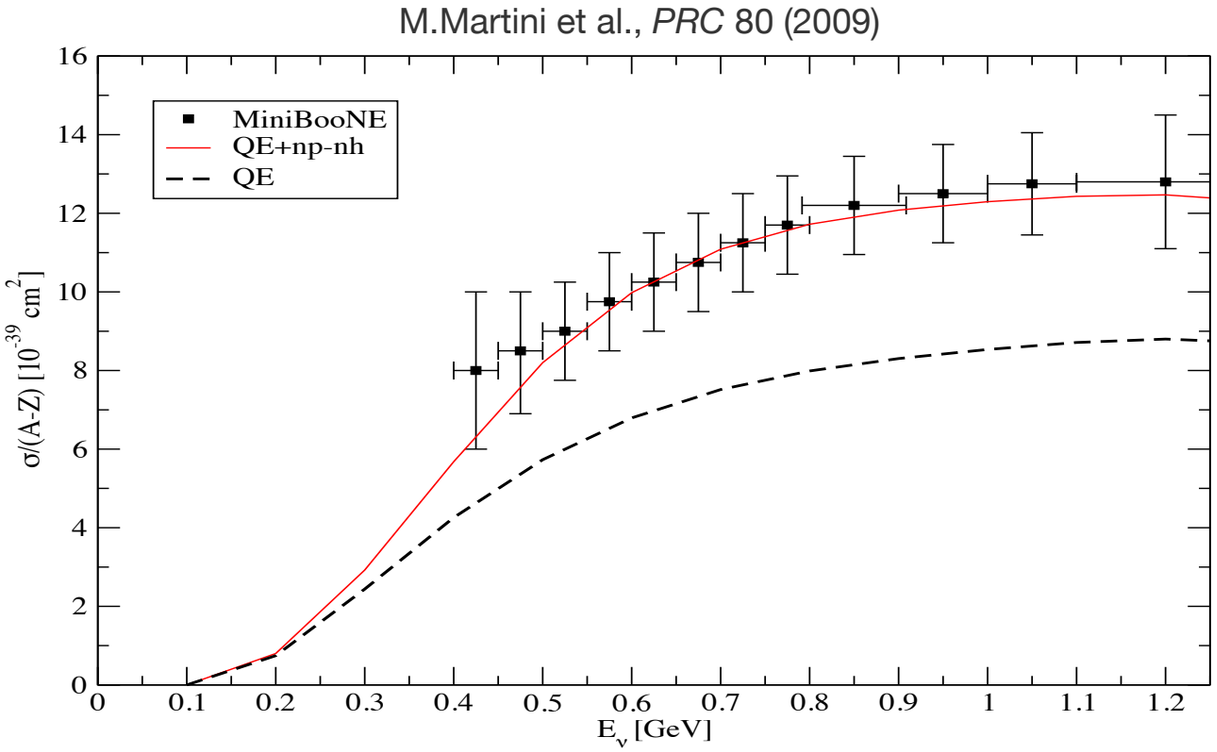

The inclusion of 2p2h contributions in the nuclear model explains the data without need of increasing the axial mass

Model comparison in the QE channel

Experimental collaborations present results in terms of final state topology
Inclusive $\nu_\mu - {}^{12}C$ CC0π cross section = no pions in the final state

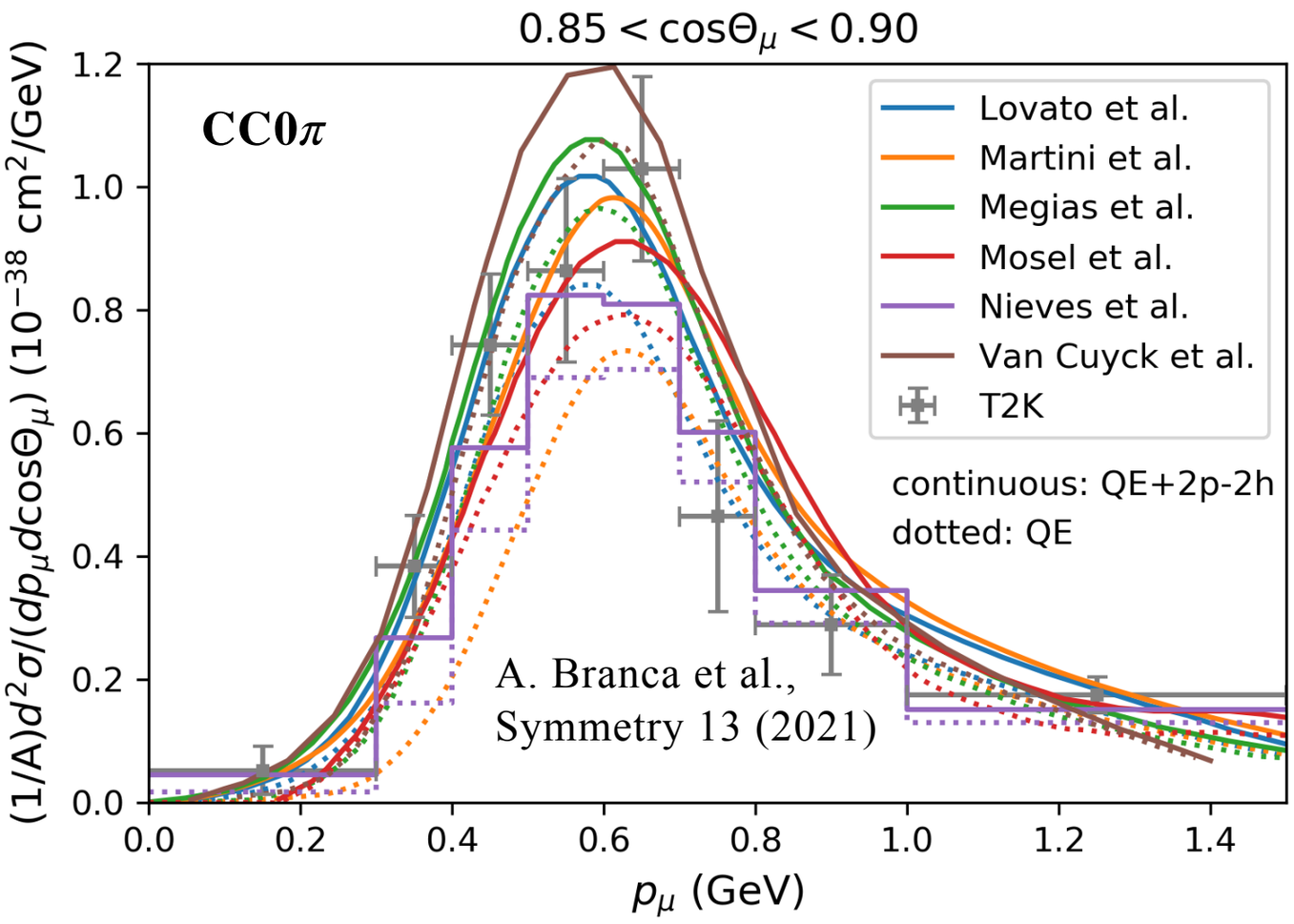

- A **quite large spread** between theory predictions is observed
- All results agree on the **important role of two-body currents** (2p2h excitations)
- However, there are **discrepancies** between 2p2h models implemented in generators
- The present experimental precision is not sufficient to discriminate between models
- **Further constraints** can be obtained from:

1. validation versus other data: **electron scattering**
2. comparison with more **exclusive data**, involving the final hadronic variables, now available from T2K, MINERvA, MicroBooNE

2p2h models in GENIE [S. Dolan et al., PRD101 (2020)]

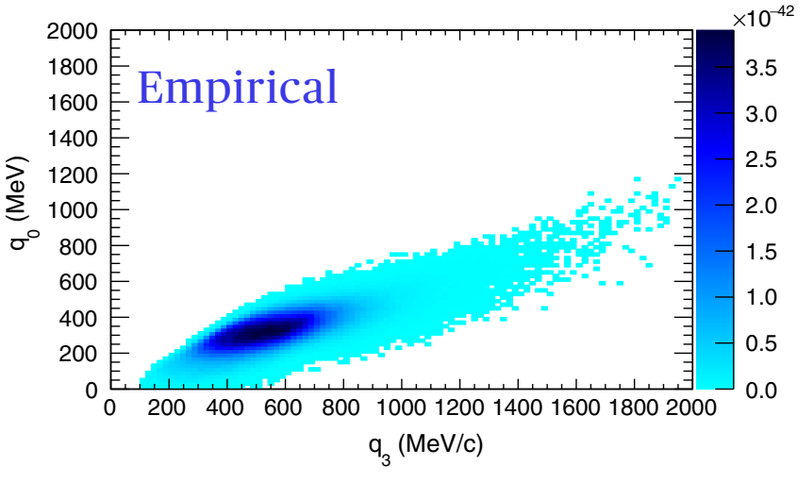

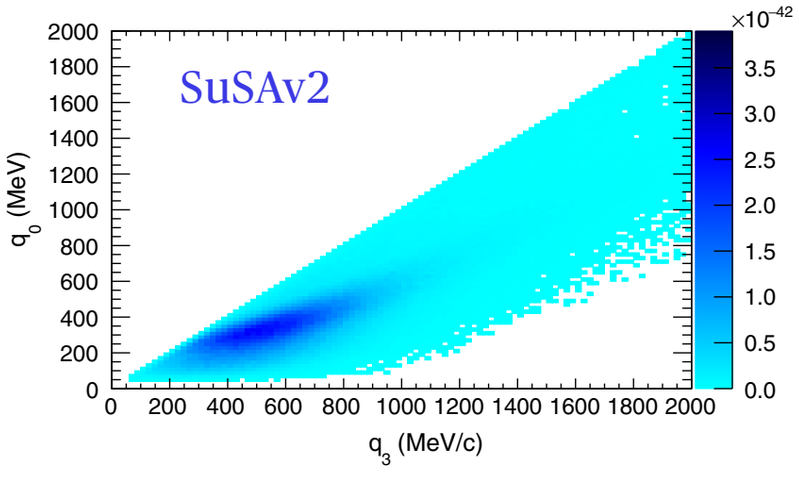

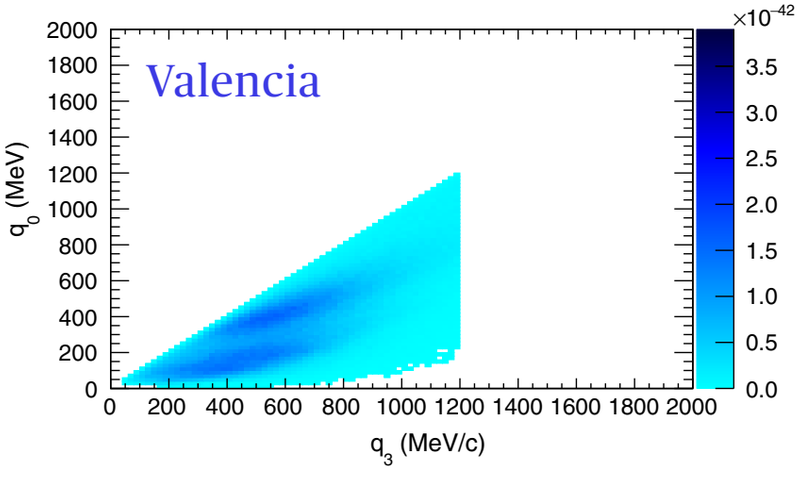

What we can learn from electron scattering

Many high quality inclusive electron scattering data exist (Saclay, Bates, Mainz, Nikhef, JLab)

- Nuclear effects in e-A and ν-A are identical, in both initial and final state.
- necessary **test** for any model for neutrino-nucleus cross sections used in MC generators
- can also be used as **input** to predict neutrino cross sections

- Two sources of difference between electron-nucleus and neutrino-nucleus cross sections

  1. different **experimental conditions:** monochromatic electron beams versus broadly distributed ν beams

  2. different **couplings and currents:** the weak cross section has a more complex structure than the electromagnetic one due to the presence of the axial current

Inclusive *l*-*A* cross section $\dfrac{d\sigma}{dk_l d\Omega_l} \sim \eta_{\mu\nu} W^{\mu\nu}$ contraction of leptonic and hadronic tensors

$$\left[\frac{d\sigma}{dk_e d\Omega_e}\right]^{(e,e')} = \sigma_{Mott}\left(V_L R_L^{\mathrm{em}} + V_T R_T^{\mathrm{em}}\right) \qquad \textbf{2 response functions}$$

$$\left[\frac{d\sigma}{dk_\mu d\Omega_\mu}\right]^{(\nu_\mu,\mu)}_{\pm} = \sigma_0\left(V_{CC}R_{CC} + 2V_{CL}R_{CL} + V_{LL}R_{LL} + V_T R_T \pm V_{T'}R_{T'}\right) \qquad \textbf{5 response functions}$$

Super Scaling Approach

1. Start from the reduced *(e,e')* cross section defined as

$$f(q,\omega;k_F) = k_F \times \frac{\left[d^2\sigma/d\omega d\Omega\right]^{(e,e')}_{exp}}{\bar{\sigma}_{eN}}$$

and plot it as function of a suitable variable $\psi \equiv \psi(q,\omega;k_F)$ for different kinematics (q) and nuclei (k_F)

scaling of first kind

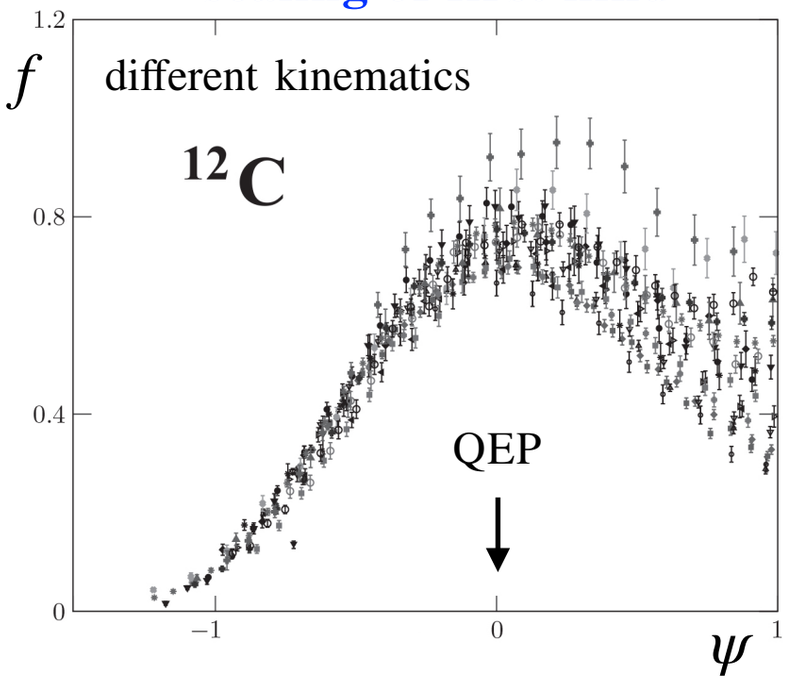

scaling of second kind

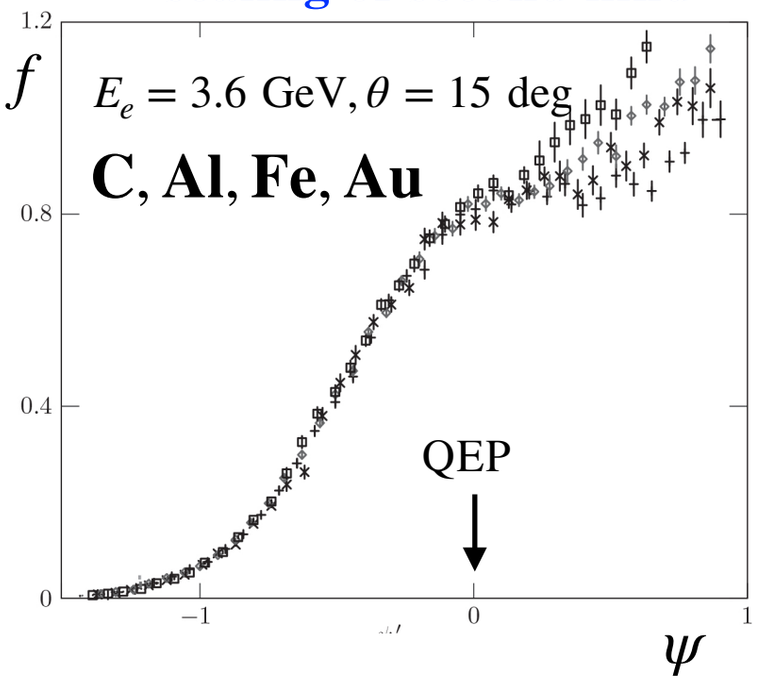

SuperScaling:
the **scaling function** *f* depends on only one **scaling variable** ψ

$$f(q,\omega;k_F) \rightarrow f(\psi)$$

Very well realised by data in the region below the QEP
$\omega < Q^2/2m_N$ and $q \gtrsim 400$ MeV

Day et al., ARNPS 40 (1990);
Donnelly and Sick, PRL82 (1999)

- The scaling function *f* encodes the nuclear dynamics, in both the initial and final state, for different kinematics and nuclei. Superscaling sets stringent constraints to nuclear models, which must reproduce it.
- The analysis of separated L and T data has shown that scaling violations mainly occur in the transverse channel and arise from non-QE processes: Δ production and 2p2h excitations

2. Use *f* to **predict the neutrino scattering cross section** (ν, l) as

$$\left[d^2\sigma/d\omega d\Omega\right]^{(\nu,l)} = \frac{1}{k_F}\bar{\sigma}_{\nu N}\ f(\psi)$$

SuSA and SuSAv2

The scaling function f can be extracted from longitudinal data or calculated within a model.

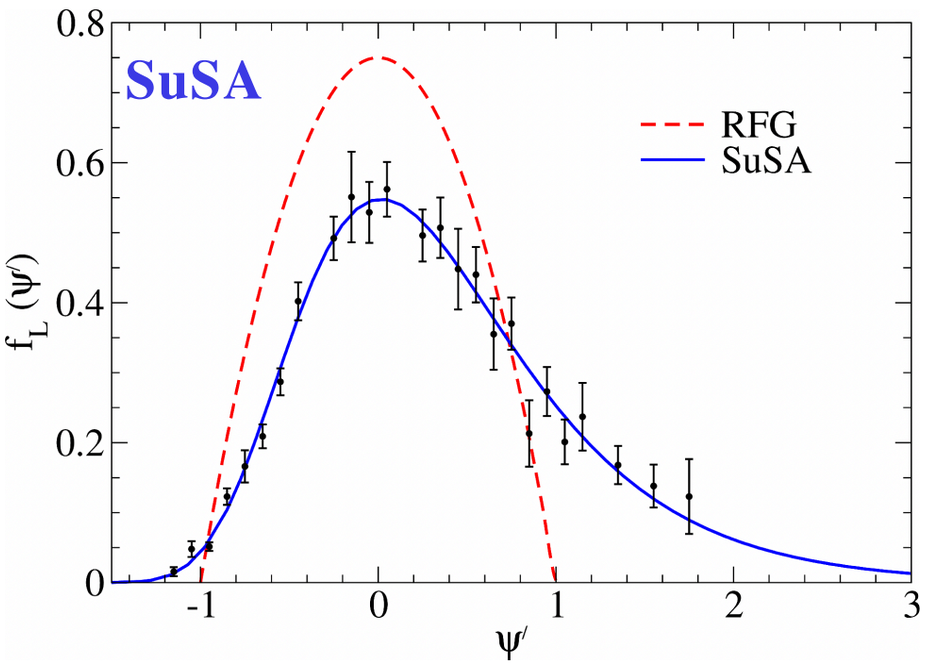

SuSA model (phenomenological)

- one scaling function extracted from longitudinal *(e,e')* data
- great improvement on the Relativistic Fermi Gas result (free relativistic nucleon correlated only by the Pauli principle)
- it is assumed that $f_L = f_T$ (assumption, true in RFG)

Amaro *et al.*, PRC71 (2005)

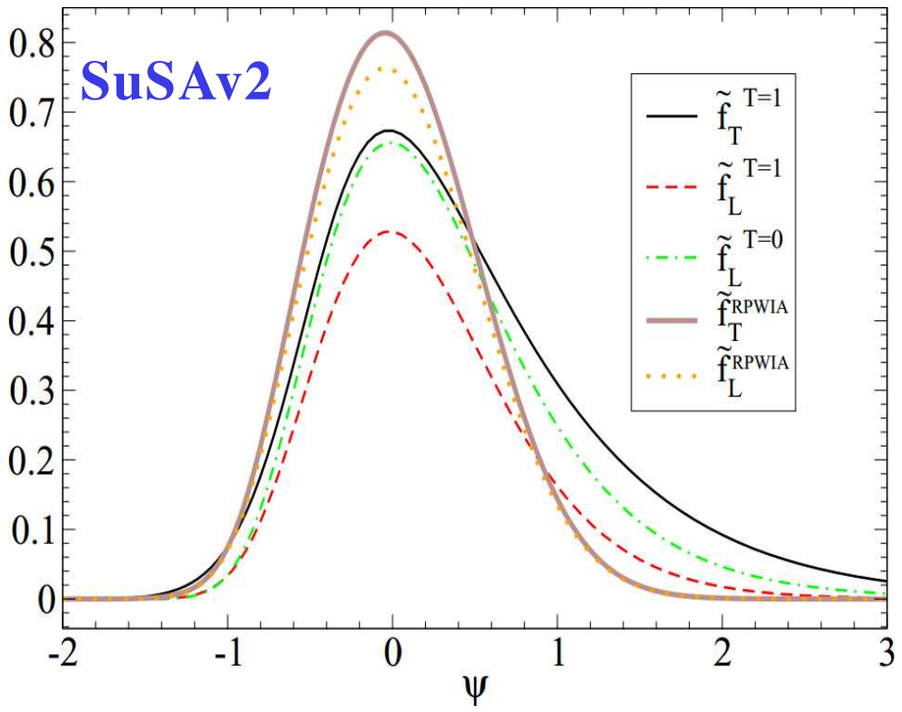

SuSAv2 model (microscopic)

- based on Relativistic Mean Field calculation
- a set of scaling functions in L,T and isospin channels
- $f_T > f_L$ in agreement with L/T separated *(e,e')* data
- parameters fitted once and for all to carbon data

Gonzalez-Jimenez *et al.*, PRC90 (2014)

The superscaling approach describes simultaneously electron and neutrino scattering

Relativistic Mean Field

The RMF model is based on the **impulse approximation (IA)**:
scattering off a nucleus = incoherent sum of single nucleon scattering processes.

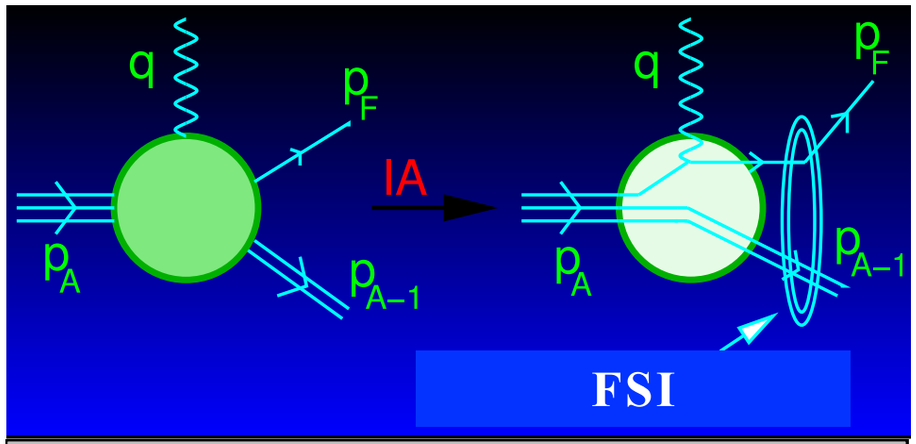

Nuclear Current $\Longrightarrow$ One-body operator

$$J^{\mu}_{N}(\omega,\vec{q}) = \int d\vec{p}\ \overline{\Psi}_{F}(\vec{p}+\vec{q})\,\hat{J}^{\mu}_{N}\,\Psi_{B}(\vec{p})$$

The nucleon wave functions are **finite nucleus** solutions of the Dirac equation with **relativistic scalar and vector potentials** obtained from a Walecka-type Lagrangian fitted to properties of nuclear radii and masses:

$$(i\gamma^{\mu}\partial_{\mu} - M - S + V)\,\psi(\vec{r},t) = 0$$

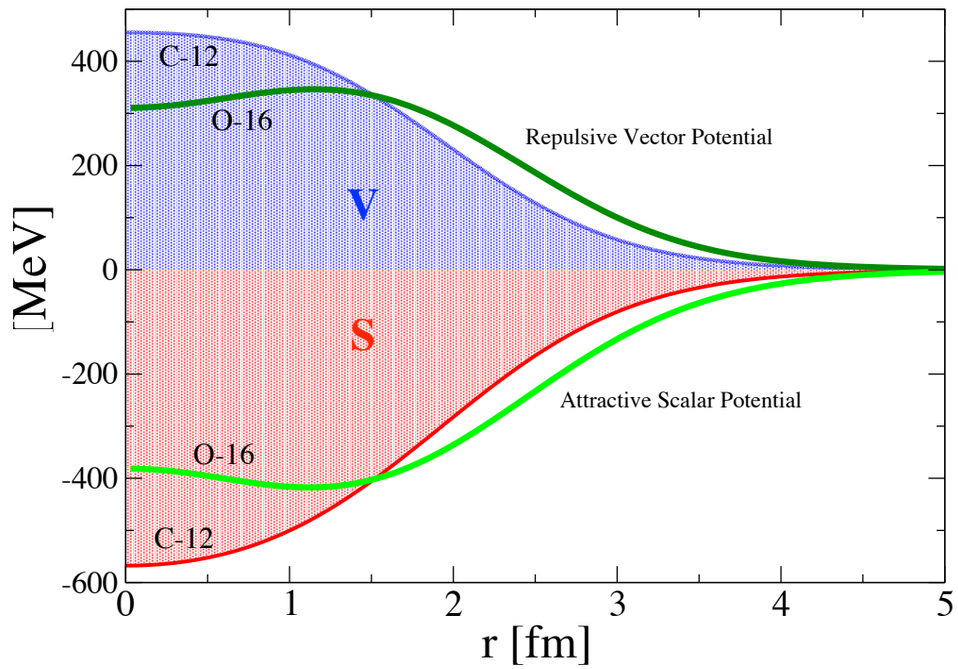

Bound wave function

$$\Psi_B = \begin{pmatrix} \phi^{up} \\ \phi^{down} \end{pmatrix} = \begin{pmatrix} \phi^{up} \\ \frac{\boldsymbol{\sigma}\cdot\mathbf{p}}{E+M+S-V}\,\phi^{up} \end{pmatrix} = \alpha u + \beta v$$

Scattered wave function

The ejected nucleon wave function is distorted by FSI with the residual nucleus.

It is a scattering solution of the Dirac equation with the same potentials used to describe the bound state.

Orthogonality is preserved: the initial and final nucleons are eigenstates of the same Hamiltonian.

Beyond the impulse approximation: Meson Exchange Currents

Two-body currents **in free space**

De Pace et al., Nucl.Phys. A726 (2003) EM
Ruiz Simo et al., J.Phys. G44 (2017) WEAK

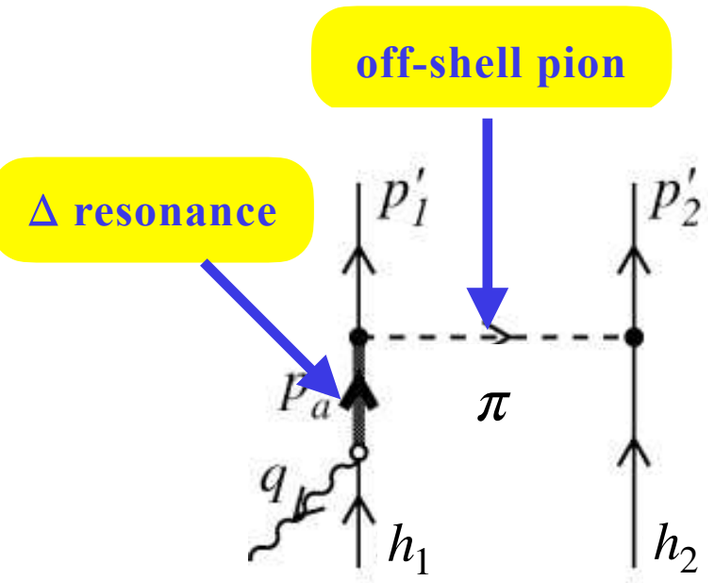

"Δ pole" (dominant)

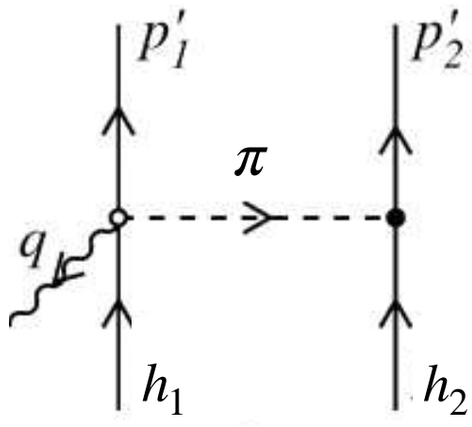

"Seagull" or "contact"

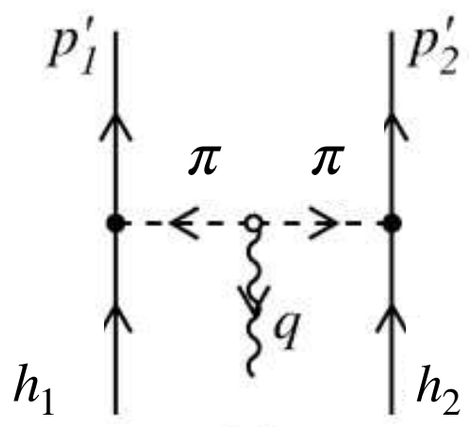

"Pion in flight"

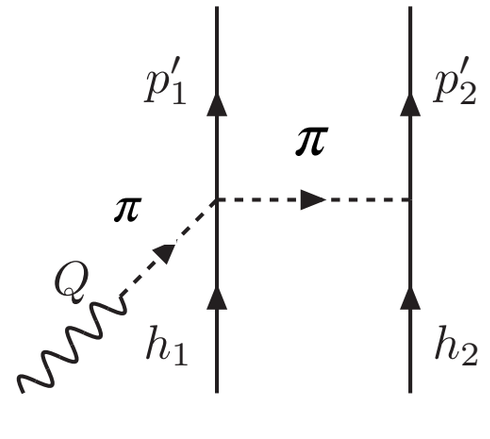

"Pion pole"
(only for neutrinos, purely axial)

In the medium, huge amount of many-body diagrams, corresponding to the excitation of **two-particle-two-hole** states.

Inclusive 2p2h hadronic tensor

$$W^{\mu\nu}_{\text{2p-2h}} = \frac{V}{(2\pi)^9}\int d^3p'_1 d^3p'_2 d^3h_1 d^3h_2 \frac{m_N^4}{E_1 E_2 E'_1 E'_2} \times r^{\mu\nu}(\mathbf{p}'_1, \mathbf{p}'_2, \mathbf{h}_1, \mathbf{h}_2)\delta(E'_1 + E'_2 - E_1 - E_2 - \omega) \times \Theta(p'_1, p'_2, h_1, h_2)\delta(\mathbf{p}'_1 + \mathbf{p}'_2 - \mathbf{h}_1 - \mathbf{h}_2 - \mathbf{q}),$$

- **fully relativistic** calculation based on **RFG**
- all many-body diagrams involving 2 pions included
- each diagram is a 7D integral+flux integration
- **np, nn and pp can be separated**

Many-body 2p2h diagrams

Direct diagrams

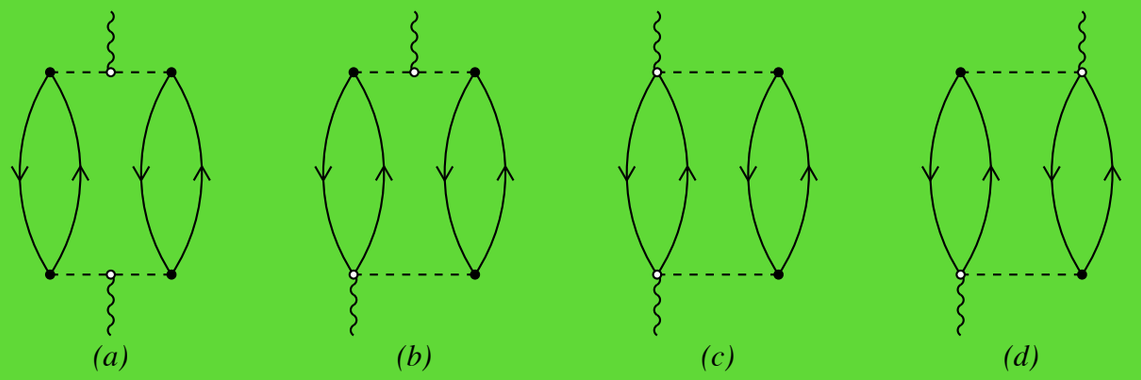

FIG. 2: The direct pionic contributions to the MEC 2p-2h response function.

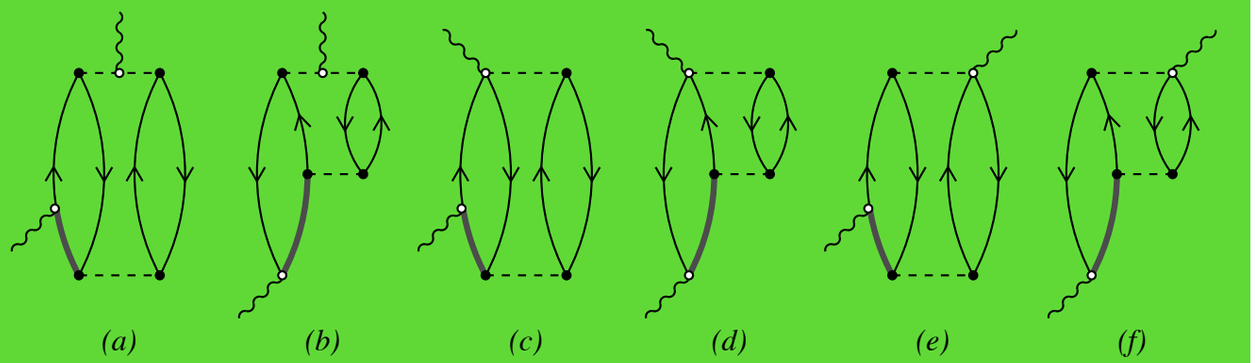

FIG. 3: The direct pionic/Δ interference contributions to the MEC 2p-2h response function.

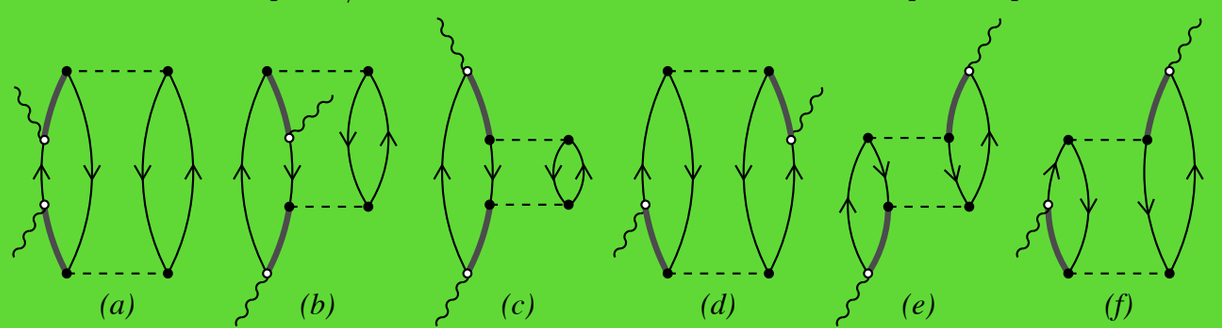

FIG. 4: The direct Δ contributions to the MEC 2p-2h response function.

Exchange diagrams

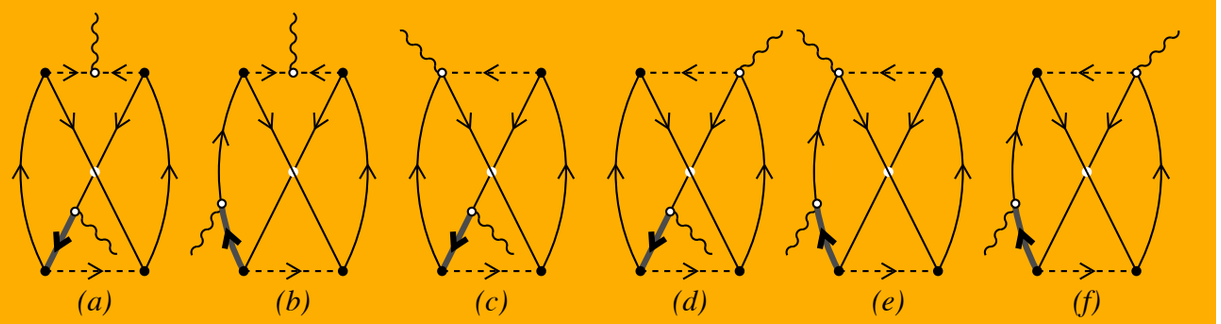

FIG. 5: The exchange pionic/Δ interference contributions to the MEC 2p-2h response function.

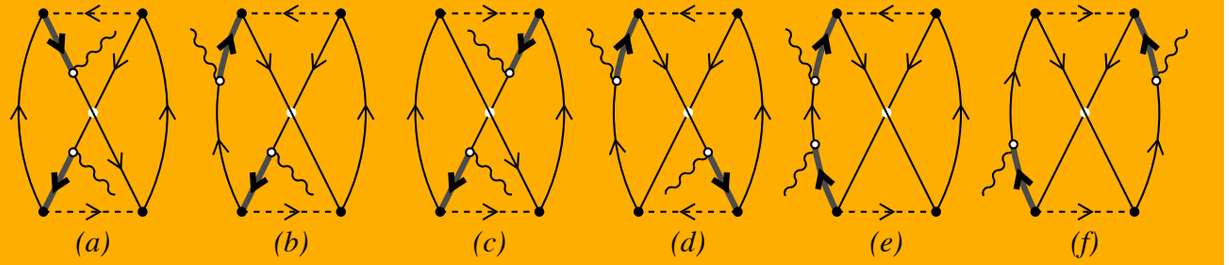

FIG. 6: The exchange Δ contributions to the MEC 2p-2h response function.

De Pace et al., NPA726 (2003)

Extension of SuSAv2 to the inelastic channel

The SuSAv2 model has been extended from the QE regime to the full inelastic spectrum by:

- introducing a **generalized scaling variable** for each invariant mass
- folding the **elementary inelastic structure functions** with the SuSA scaling variable

$$R^K_{QE}(q,\omega) \propto f(\psi)\, U^K(q,\omega) \;\rightarrow\; R^K_{inel}(q,\omega) \propto \int_{W_{min}}^{W_{max}} dW_X f(\psi_X)\, U^K_{inel}(q,\omega)$$

U^K_{inel} are single-nucleon functions containing the transition form factors:

- for **electron scattering** one can use phenomenological parametrizations of the inelastic structure functions w_1, w_2 [Bodek and Ritchie PRD 24 (1981), Bosted and Christy PRC76 (2008), PRC81 (2010)]

- the extension to the **weak channel** is limited by the poor knowledge of the three structure functions w_1, w_2, w_3 in the inelastic region beyond the Δ-resonance production. Parametrizations across the full energy spectrum are not available. One has to rely on models.

MBB et al., PRC69 (2004), Gonzalez-Rosa et al., PRD105 (2022)

Validation: SuSAv2 comparison with (e,e') data

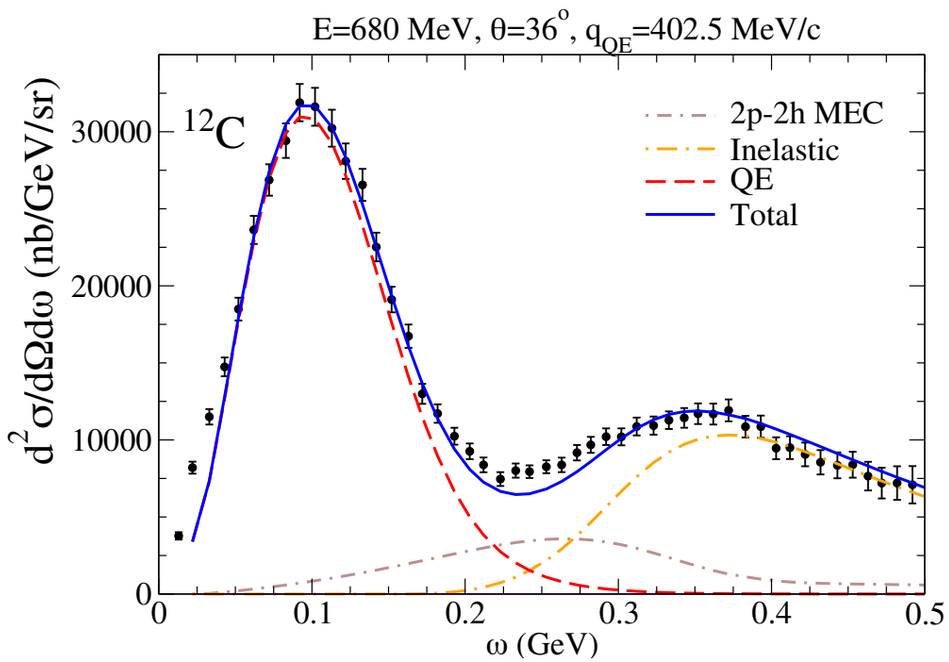

Megias *et al.*, PRD94 (2016)

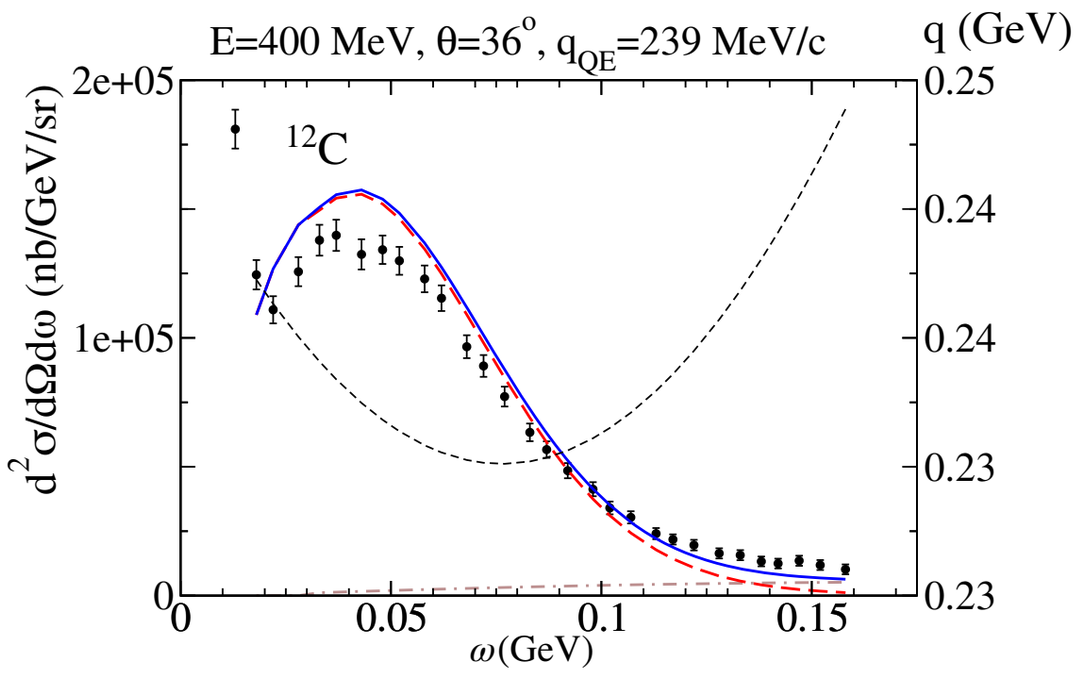

Data: Barreau, NPA402 (1983)

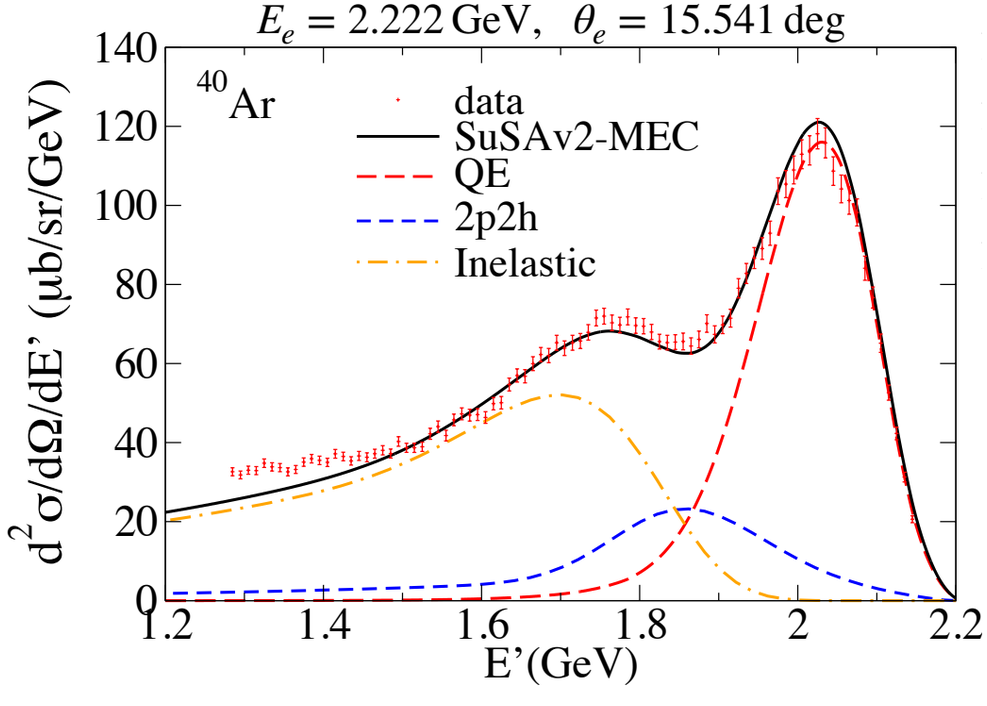

MB *et al.*, PRC99 (2019)

Data: Dai, PRC98 (2018)

Good agreement with data for different nuclei in a wide kinematical region, with the exception of the very low q regime, where the superscaling approach and IA fail and collective effects dominate.

SuSAv2 comparison with (ν_μ, μ) CC0π data

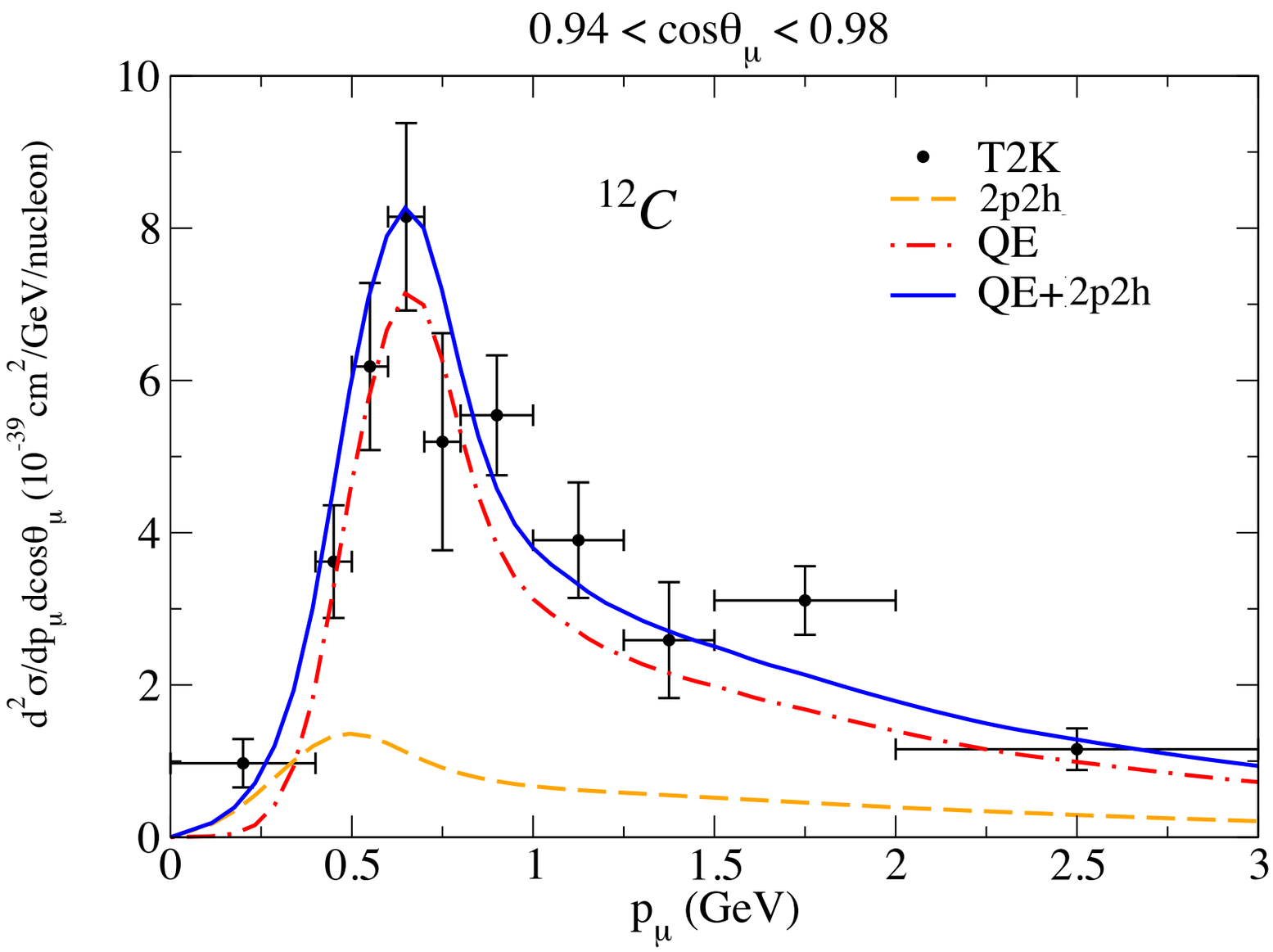

Megias *et al*., JPG46 (2019)

data: T2K coll., PRD 97 (2018)

CC0π

Some more examples: neutrino and antineutrino cross sections, different experiments, kinematics and nuclei

In general good agreement with data (but large error bars)

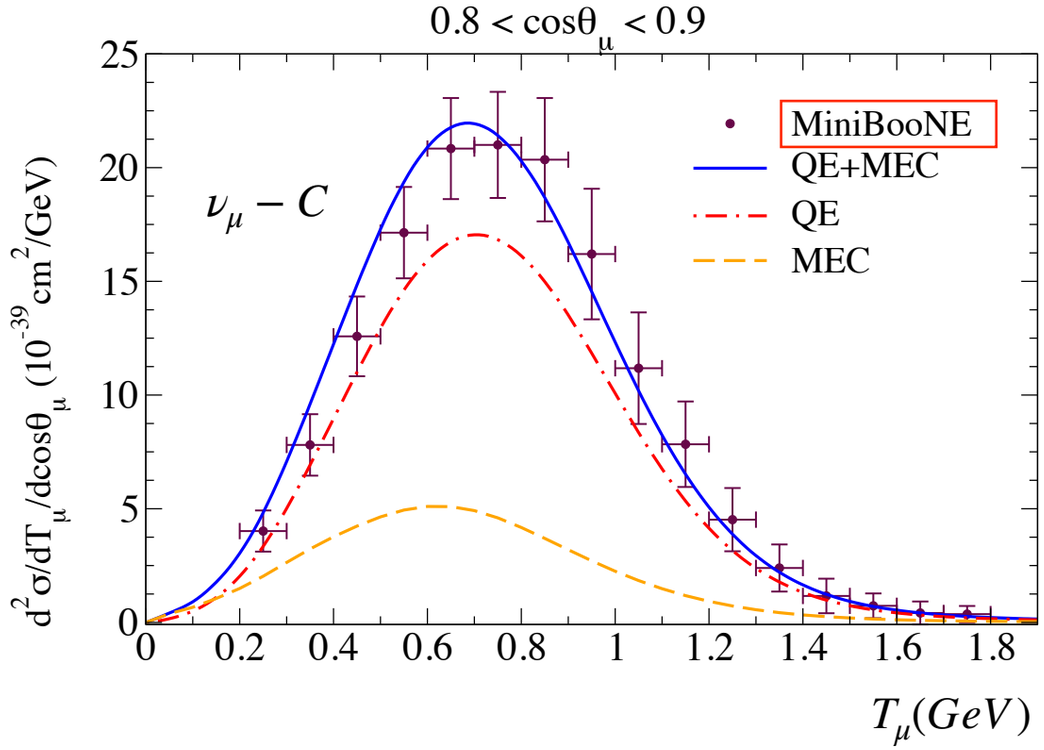

Megias *et al.*, PRD94 (2016)

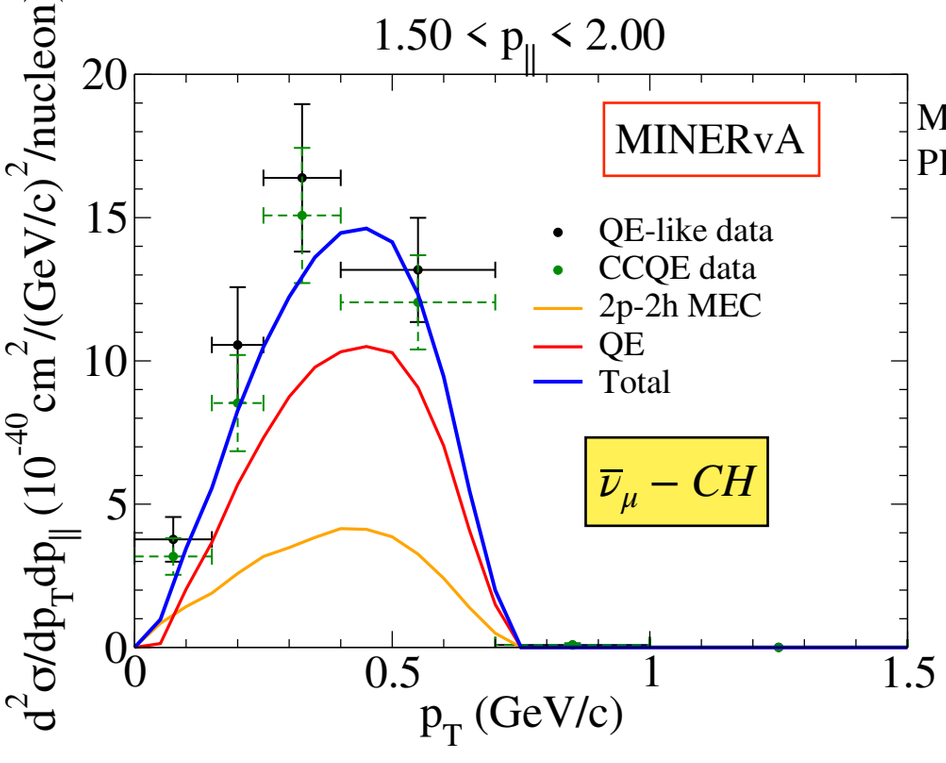

Megias *et al.*, PRD 99 (2019)

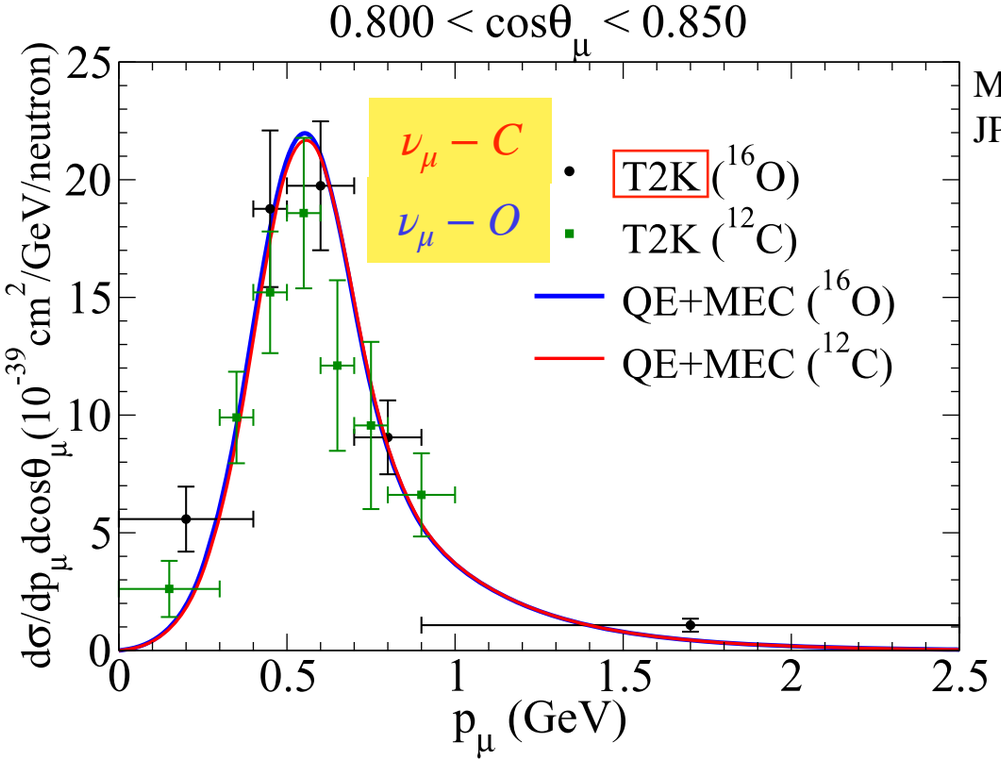

Megias *et al.*, JPG46 (2019)

Implementation in GENIE

S. Dolan *et al.*, PRD101 (2020)

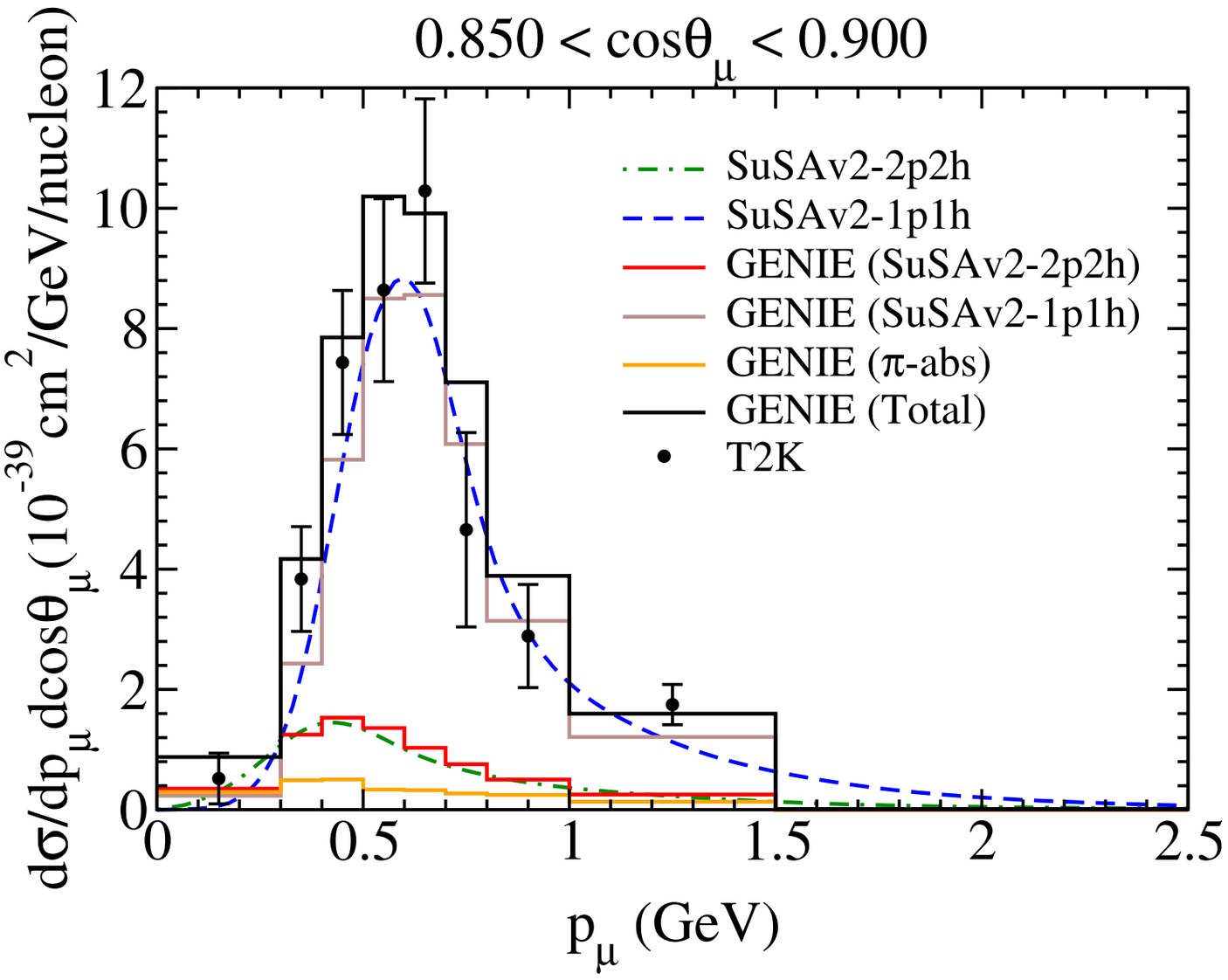

The SuSAv2 model is now implemented in GENIE, in both the QE and 2p2h channels

Check: for the cross section versus the muon variables, the results of the implementation (histograms) are in good agreement with the original calculation (curves).

However, the model was implemented by using the **inclusive hadronic tensor** under some assumptions, not necessarily consistent with the model, but unavoidable since **the SuSA model is intrinsically inclusive**.

The implementation must be improved starting from the complete semi-inclusive results. Very few microscopic calculations of the semi-inclusive neutrino-nucleus cross section exist at present.

Neutrino-nucleus semi-inclusive scattering

Many recent semi-inclusive data has been published by T2K, MINERvA, MicroBooNE
The outgoing lepton and one ejected nucleon are detected in coincidence

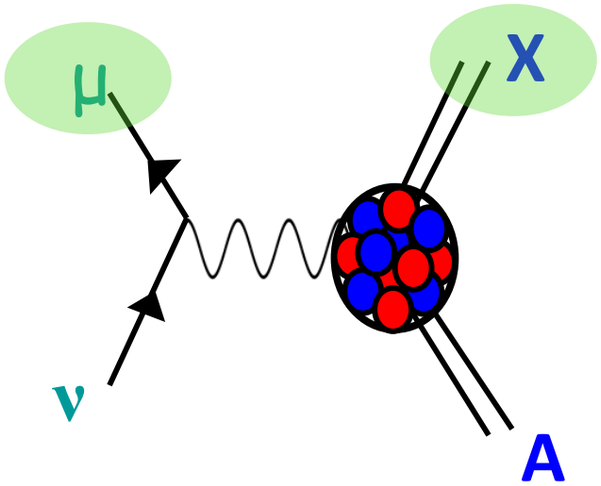

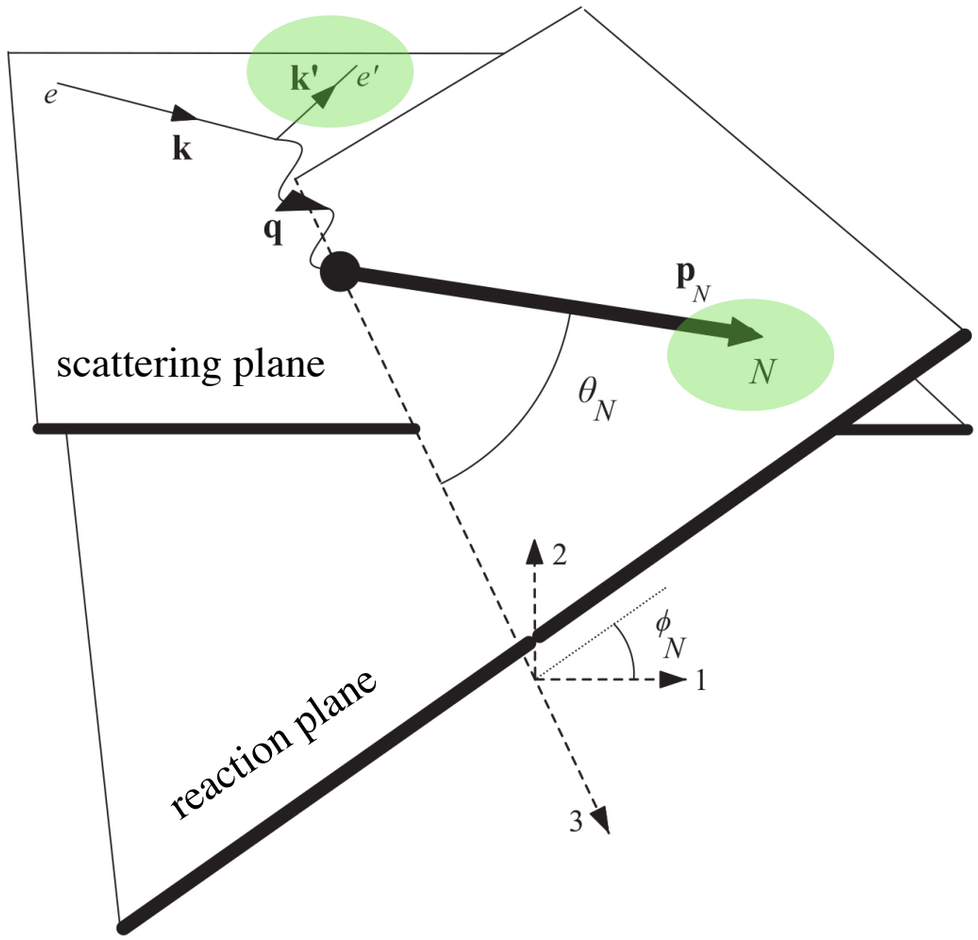

Spectral function

$$\left\langle \frac{d^6\sigma}{dk'd\Omega' dp_p d\Omega_p} \right\rangle = \int_0^\infty dk \frac{\Phi_\nu(k)}{k} K_0 S(p_m, E_m) \mathcal{F}^2 \theta(E_m - E_s)$$

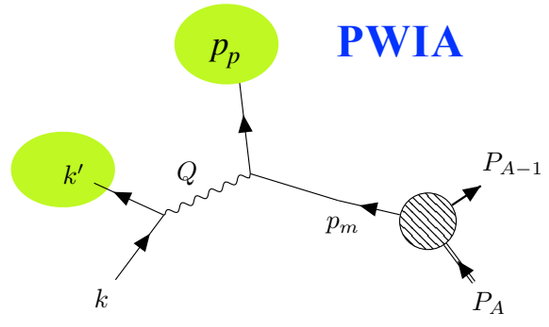

Key quantity: **spectral function,** describing the joint probability of finding a nucleon of momentum p_m in the nuclear g.s. A and reaching final states in the daughter nucleus A-1 characterised by missing energy E_m

$\mathbf{p}_m = \mathbf{q} - \mathbf{p_N} = \mathbf{p_{A-1}}$ missing momentum

$E_m = \omega - T_N - T_{A-1}$ missing energy

State of the art

$$S_{\text{Rome}}(p_m, E_m) = S_{\text{SP}}(p_m, E_m) + S_{\text{corr}}(p_m, E_m)$$

$S_{\text{SP}}(p, E) = \sum_n Z_n |\phi_n(p) F(E_m - E)|^2$ shell contribution from (e,e'p) data, accounting for ~80% of the strength

$S_{\text{corr}}(p, E)$ high missing energy and momentum tail due to NN correlation extrapolated from nuclear matter using LDA [Benhar, Fabrocini, Fantoni, Sick et al., NPA 579 (1994)]

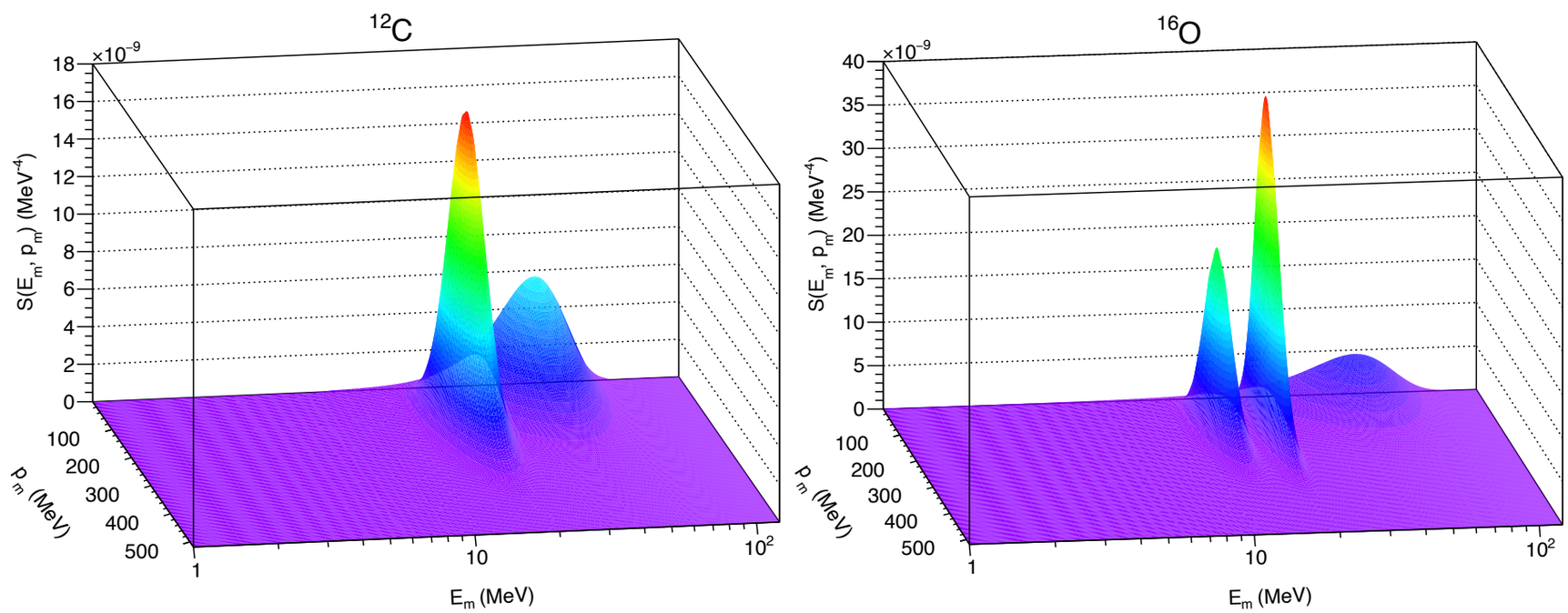

Argon

^{40}Ar is the target in experiments using Liquid Argon Time Projection Chambers technique

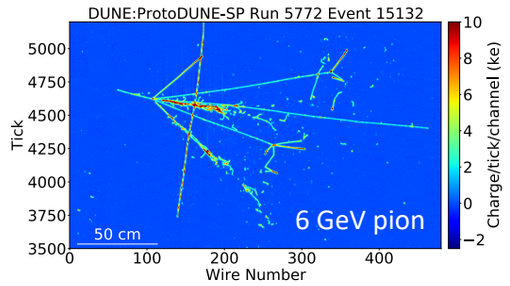

α	E_κ (MeV)	σ_κ (MeV)	S_κ
$1s_{1/2}$	55 ± 6	30 ± 15	0.9 ± 0.15
$1p_{3/2}$	39 ± 4	12 ± 6	0.9 ± 0.15
$1p_{1/2}$	34 ± 3	12 ± 6	0.9 ± 0.15
$1d_{5/2}$	23 ± 2	5 ± 3	0.75 ± 0.15
$2s_{1/2}$	16.1 ± 1.6	5 ± 3	0.75 ± 0.15
$1d_{3/2}$	16.0 ± 1.6	5 ± 3	0.75 ± 0.15
$1f_{7/2}$	9.869 ± 0.005	5 ± 3	0.75 ± 0.15

- positions E_k from **RMF calculation**

- widths σ_k from **JLab (e,e'p) experiment** on Ar [Jiang et al., PRD 105, 2022]

- spectroscopic factors S_k from phenomenology

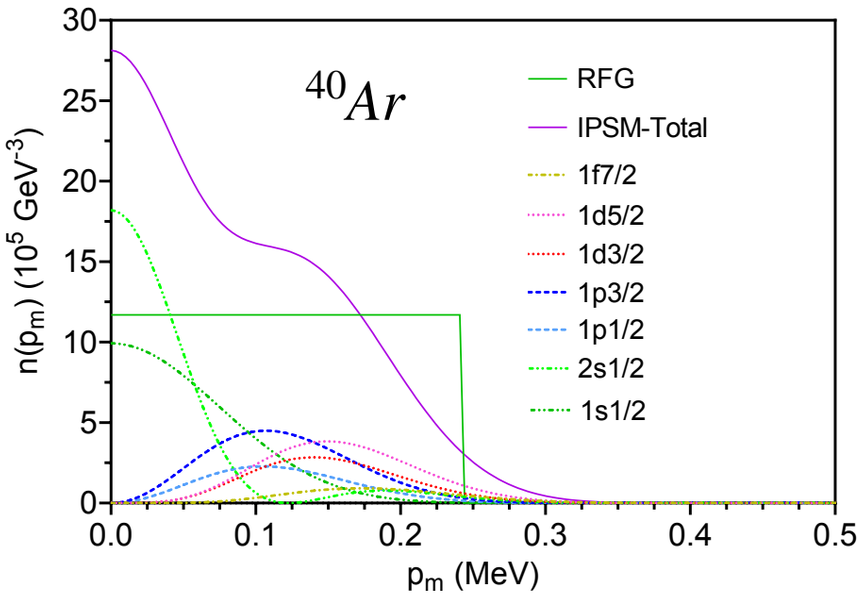

$$n(p_m) = \int_0^\infty dE_m \, S(p_m, E_m)$$

Missing energy distribution for the 22 neutrons of ^{40}Ar

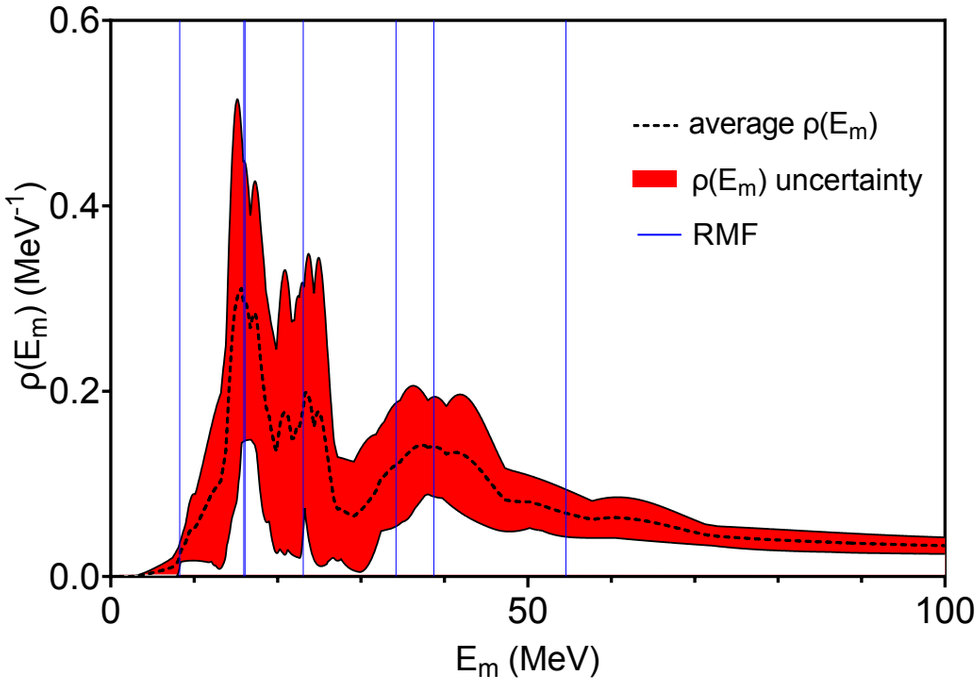

Conservative error bands are assigned to the SF parametrization, related to the extraction from (e,e'p) data

$^{40}Ar(\nu_\mu, \mu^- p)^{39}Cl$	DUNE flux	$d^6\sigma$	six-differential	$k' = 1.5\,\text{GeV}, \theta_\mu = 30^0, \phi_N^L = \pi$

Relativistic Plane Wave Impulse Approximation (no FSI included)

Striking differences in the cross section due to initial state physics described by different spectral functions. The precise knowledge of the SF is crucial for a reliable modelling of semi-inclusive reactions.

Relativistic Fermi Gas

$$S_{\text{RFG}}(p_m, E_m) = \theta(p_F - p_m)\,\delta\left(E_m - \sqrt{p_m^2 + m_N^2}\right)$$

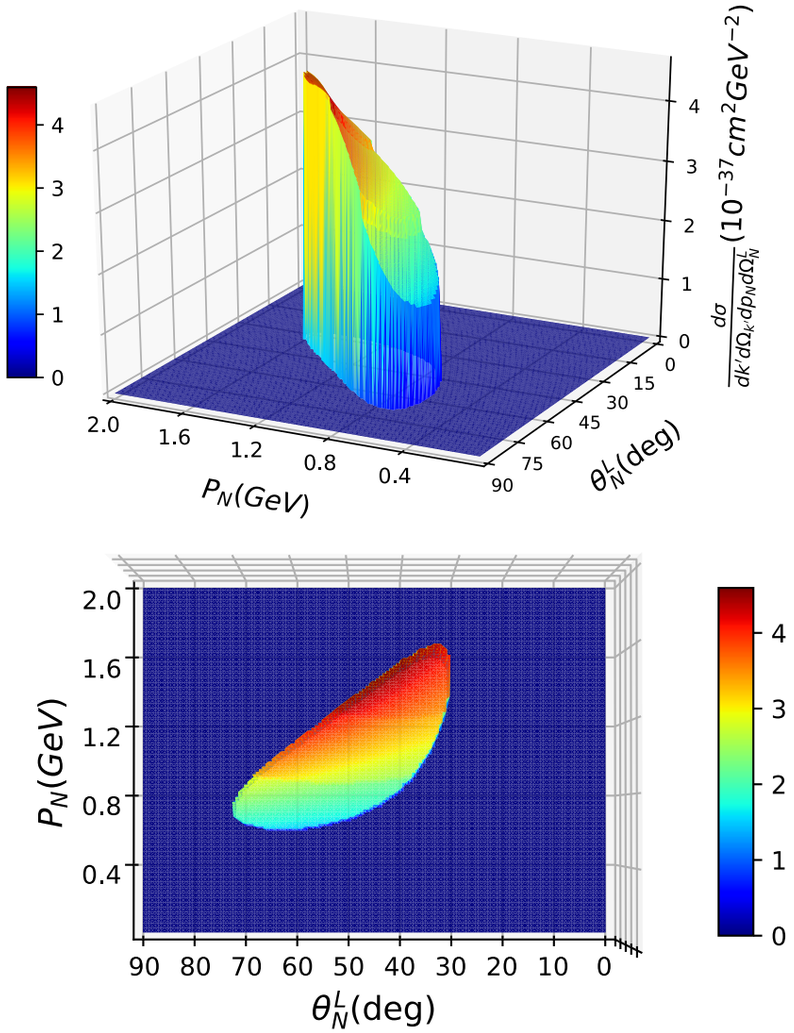

Independent Particle Shell Model

$$S_{\text{IPSM}}(p, E) = \sum_{nlj} (2j+1)\; n_{nlj}(p)\; \delta(E - E_{nlj})$$

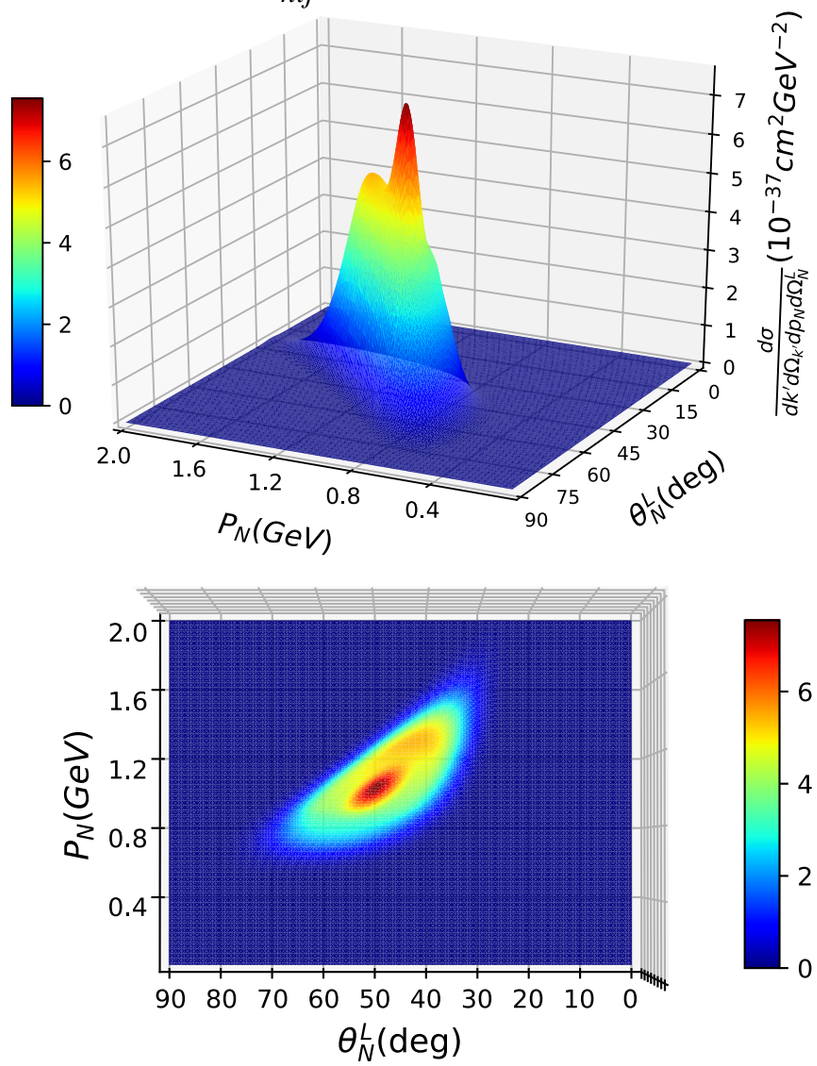

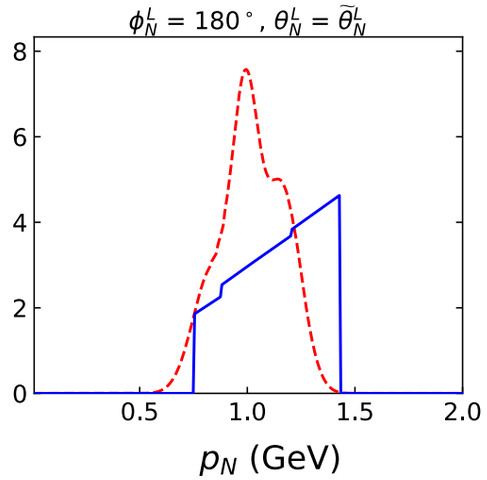

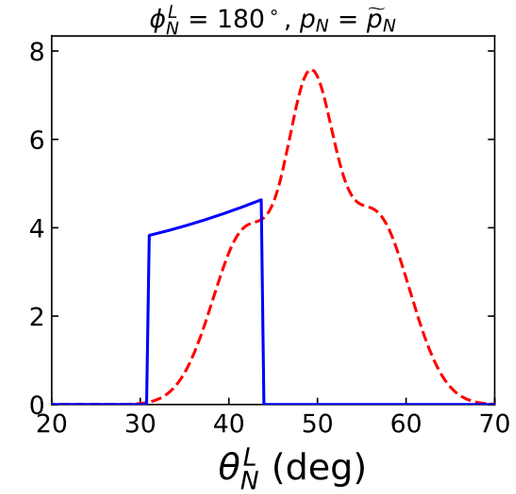

IPSM

RFG

J.M. Franco-Patiño *et al.*, PRC 102, 064626 (2020)

Final-state interactions

RPWIA →RDWIA

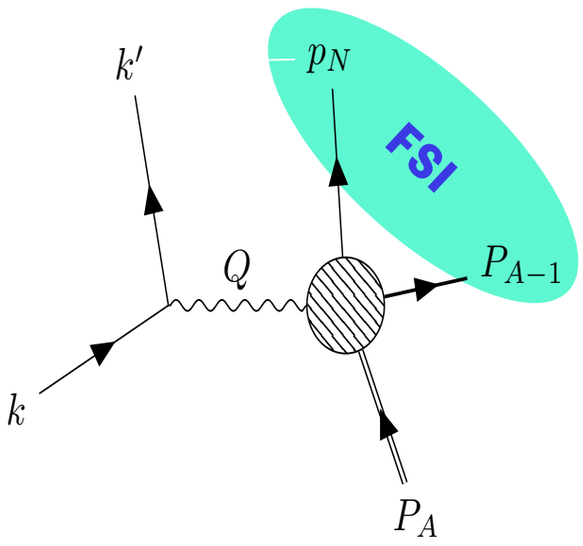

^{12}C

R. Gonzalez-Jimenez *et al.*, Phys.Rev.C 101 (2020) 1, 015503

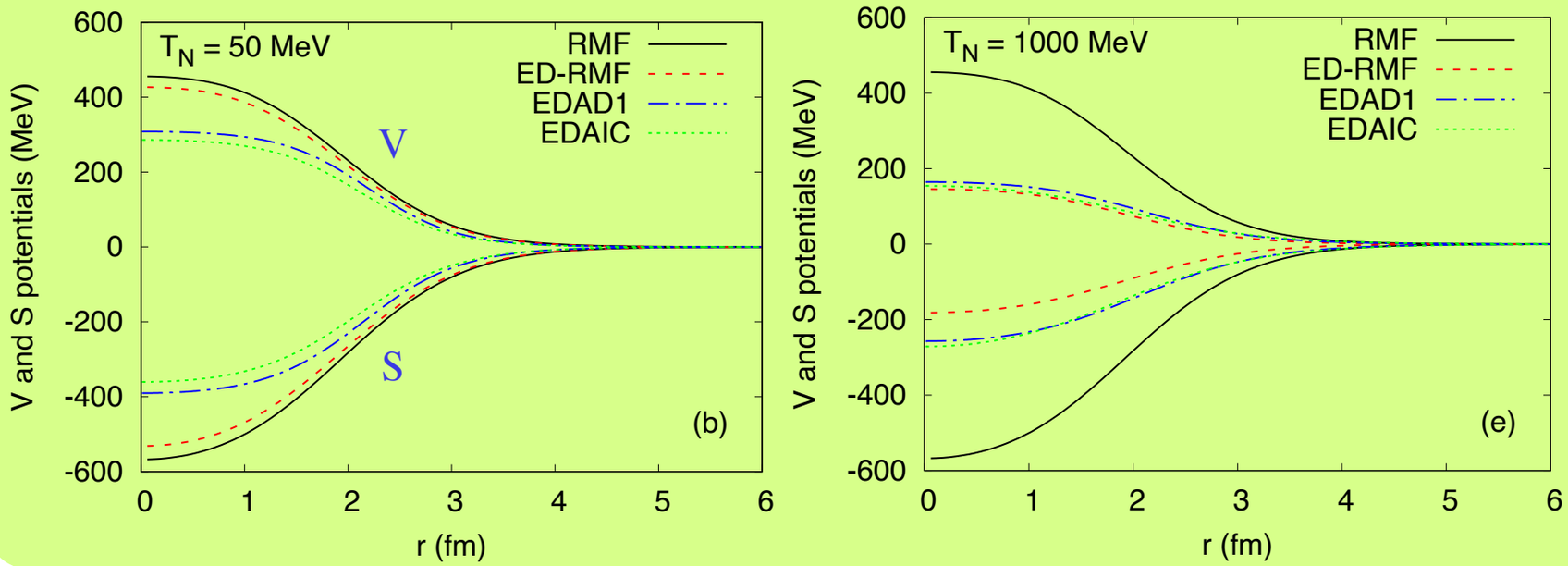

FSI between the knocked-out nucleon and the residual nucleus can be treated using different approaches:

- **Optical Potentials,** energy-dependent A-(in)dependent **EDAD** (**EDAI**)

  ROP: full complex relativistic OP, the Im part accounts for loss of flux to inelastic channels, used e.g. in (e,e'p) studies where the elastic channel is isolated

  rROP: only real part of the ROP, more appropriate to describe inclusive reactions where all channels contribute to the signal. Orthogonality issues for low momentum transfers.

- **Relativistic Mean Field** (**RMF**): real energy-independent potentials. Orthogonality is preserved but potentials are too strong at high energy, where the RPWIA should be recovered.

- **Energy-Dependent Relativistic Mean Field** (**ED-RMF**)**:** RMF suppressed at high energy by a function $f(T_N)$ fitted to (e,e') data. This approach is numerically equivalent to SuSAv2 for inclusive reactions but, unlike SuSAv2, is applicable also to the semi-inclusive case.

Some theory/data comparison for semi-inclusive $\nu - A$ scattering

J.M. Franco-Patiño et al.,

Phys. Rev. D 104 (2021)
Phys. Rev. D 106 (2022)
e-Print: 2304.01916

Data:

	Experiment	Neutrino energy	Target
Abe et al., PRD 98 (2018)	**T2K**	$E_\nu \sim$ **0.6 GeV**	**CH**
Lu et al., PRL 121 (2018); Cai et al., PRD 101 (2020)	**MINERvA**	$E_\nu \sim$ **3 GeV**	**CH**
Abratenko et al., PRD 102 (2020); PRL 125 (2020)	**MicroBooNE**	$E_\nu \sim$ **0.6 GeV**	**Ar**

T2K

1μCC0πNp with at least one proton in the final state with momentum above 0.5 GeV

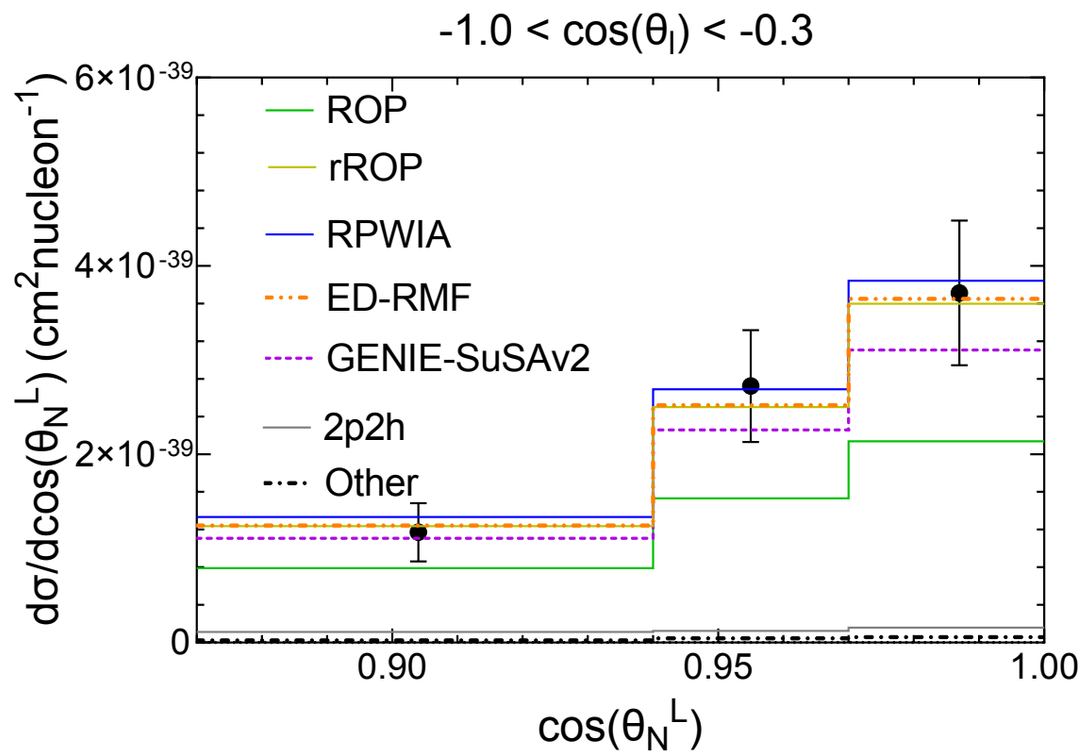

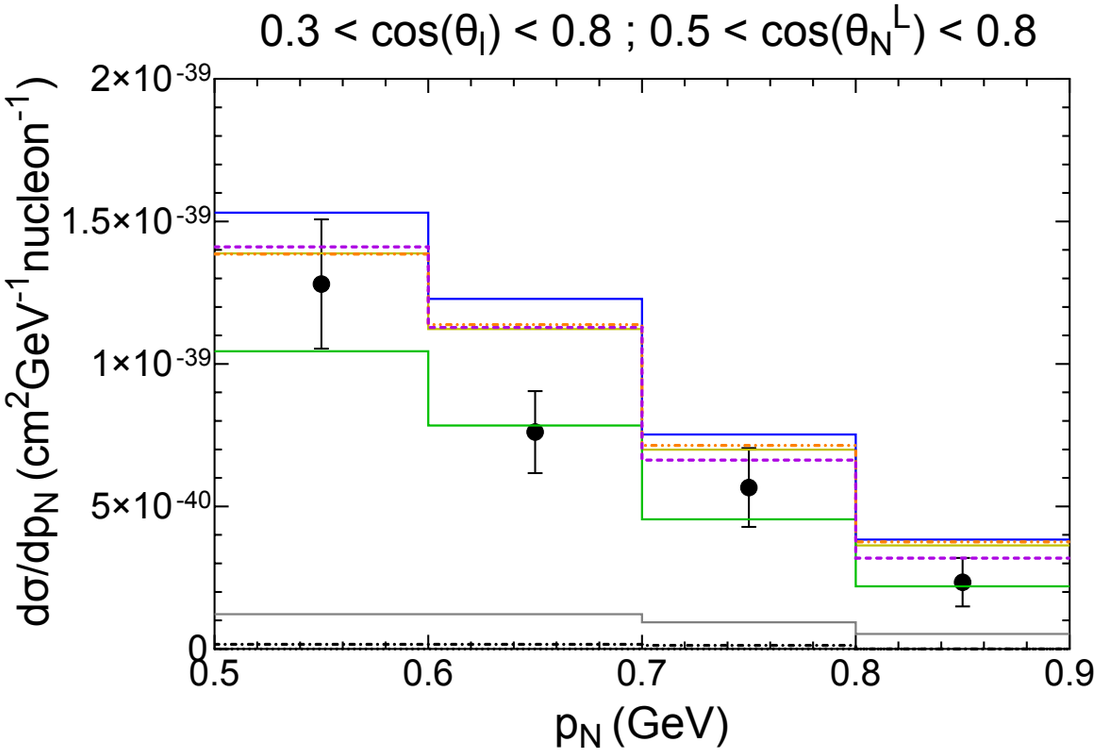

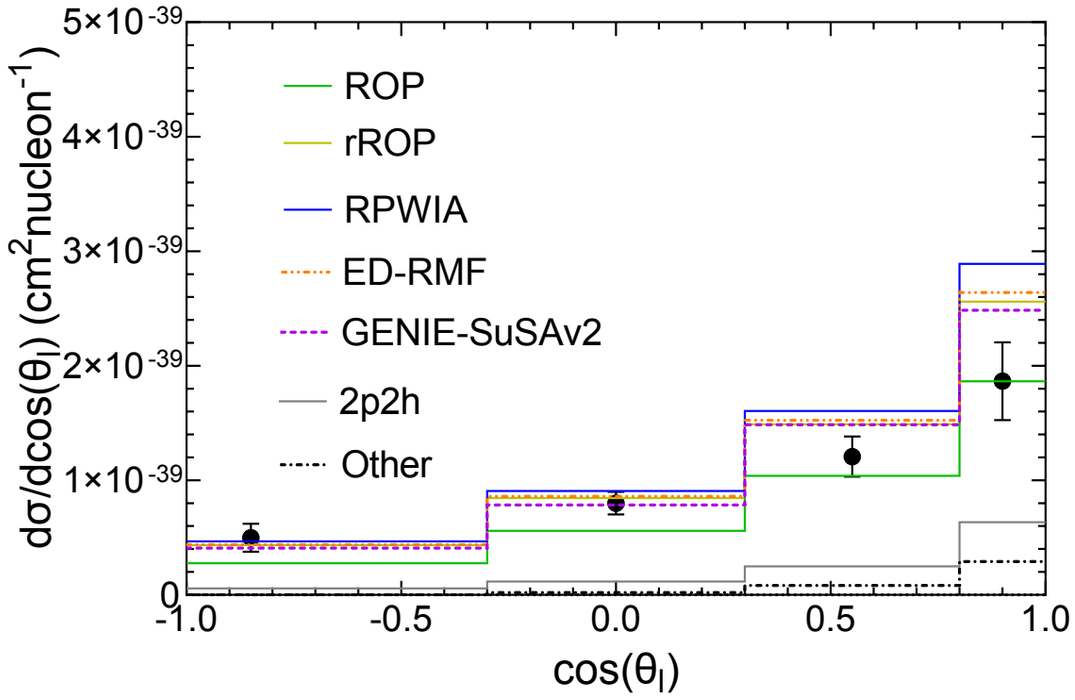

No clear trend emerges from the model/ data comparison at different lepton and proton kinematics

2p2h and "Other" (pion emission followed by re-absorption) from GENIE simulation

Microscopic calculations for these processes ares till missing

Transverse Kinematic Imbalance (TKI)

Data are often represented in terms of new variables devised to enhance sensitivity to nuclear effects

Lu et al., PRC94, 015503 (2016)

$$\delta p_T = |\delta \mathbf{p_T}| = |\mathbf{k'_T} + \mathbf{p_{N,T}}| \ ,$$

$$\delta \alpha_T = \arccos\left(-\frac{\mathbf{k'_T}\cdot\delta\mathbf{p_T}}{|\mathbf{k'_T}|\ |\delta\mathbf{p_T}|}\right) \ ,$$

$$\delta \phi_T = \arccos\left(-\frac{\mathbf{k'_T}\cdot\mathbf{p_{N,T}}}{|\mathbf{k'_T}|\ |\mathbf{p_{N,T}}|}\right) \ ,$$

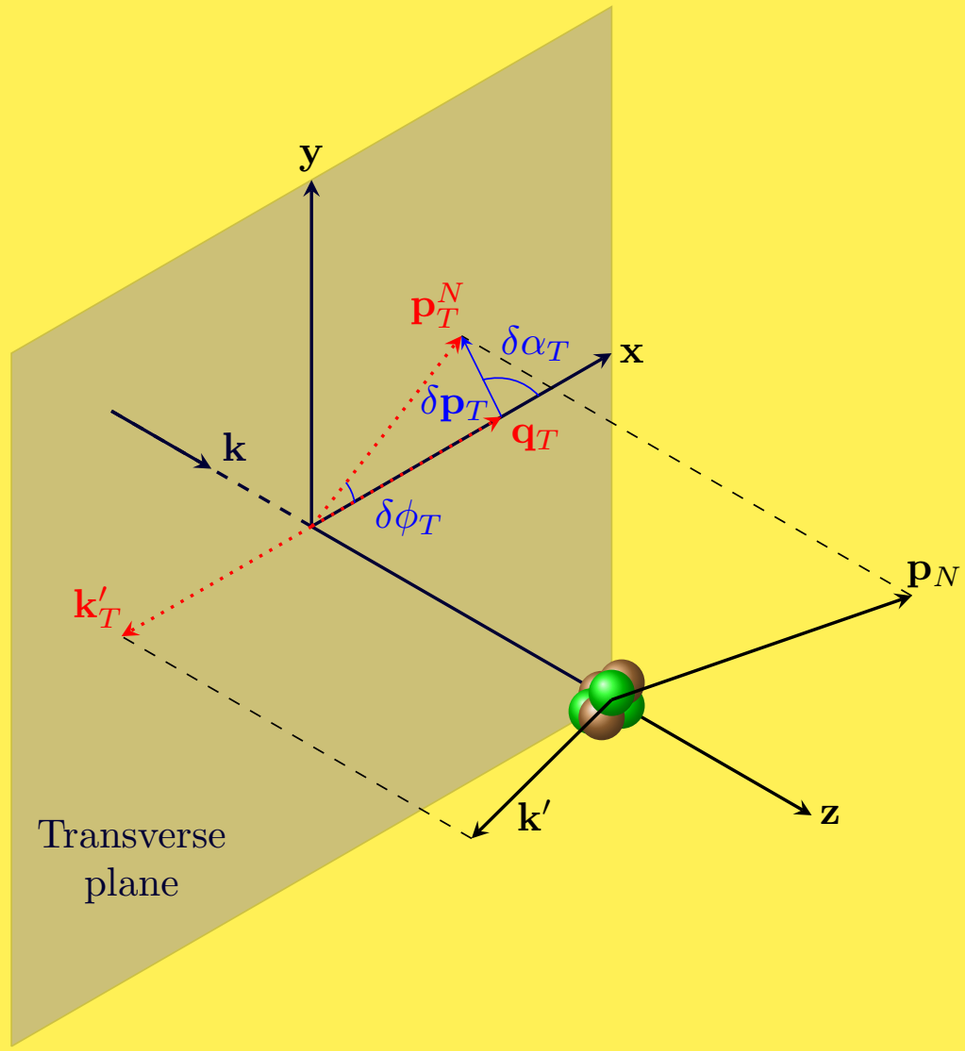

On a free nucleon at rest $\mathbf{k'_T} = -\mathbf{p_{N,T}}$

$\delta p_T = \delta\phi_T = 0$ —> peaked distribution

$\delta\alpha_T$ undefined —> flat distribution

Deviations from these behaviours "measure" nuclear effects with minimum dependence upon the neutrino energy:

δp_T distribution is related to the nucleon momentum distribution

$\delta\alpha_T$ sensitive to non-QE effects (2p2h) and FSI

T2K

TKI distributions

$1\mu CC0\pi Np$ $p_N > 500$ MeV

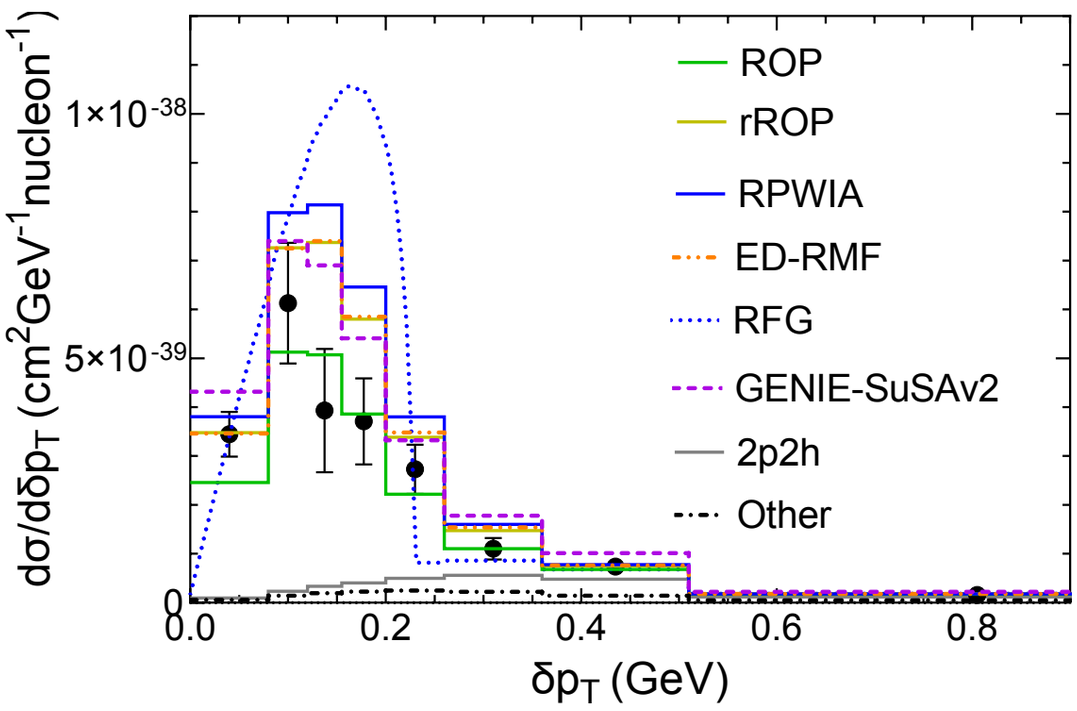

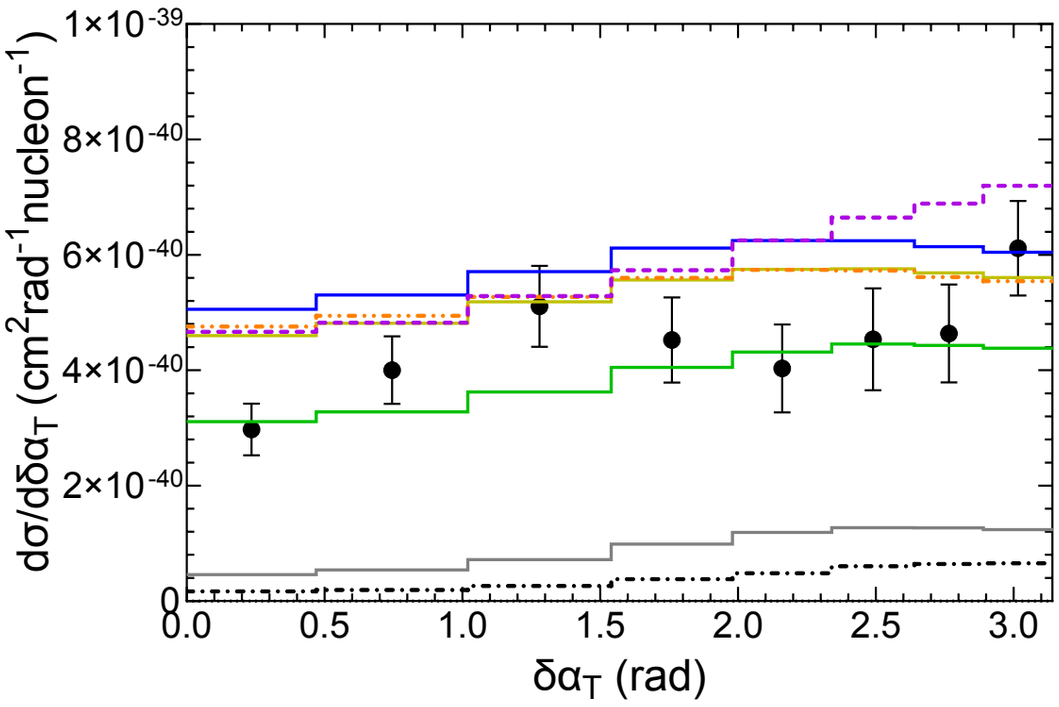

- In the absence of FSI, the δp_T distribution is related to the nucleon momentum distribution: the RFG is clearly ruled out
- The role of FSI is sizeable, especially in the ROP approach
- 2p2h mainly affect the high momentum tail

- ROP describes better the data versus $\delta\alpha_T$
- The departure from flat distribution is determined by the 2p2h contribution
- No model is able to reproduce the oscillatory behaviour of data

MINERvA

1μCC0πNp with at least one proton in the final state

Natural lepton and proton variables

kinematic restrictions

MINERνA	k' (GeV)	$\cos\theta_l$	p_N (GeV)	$\cos\theta_N^L$	ϕ_N^L (°)
	1.5-10	> 0.939	0.45-1.2	> 0.342	-

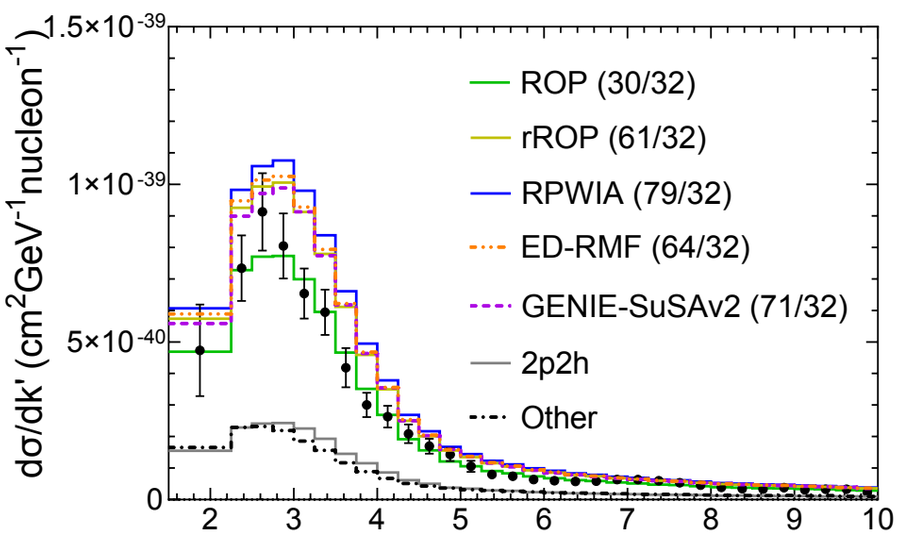

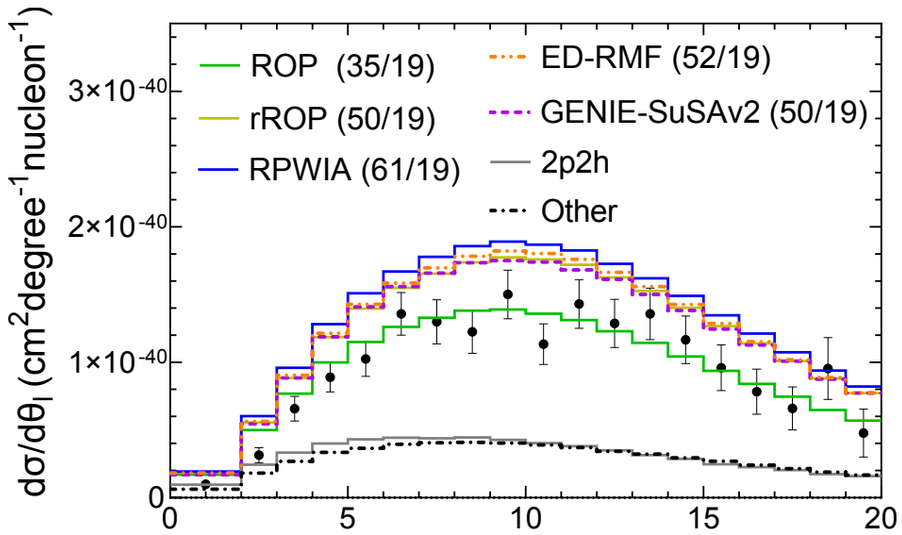

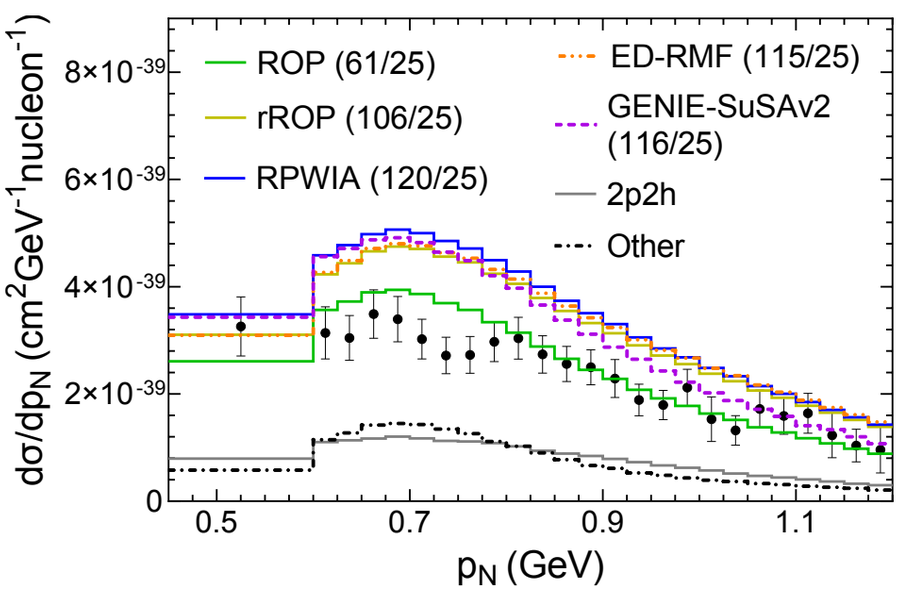

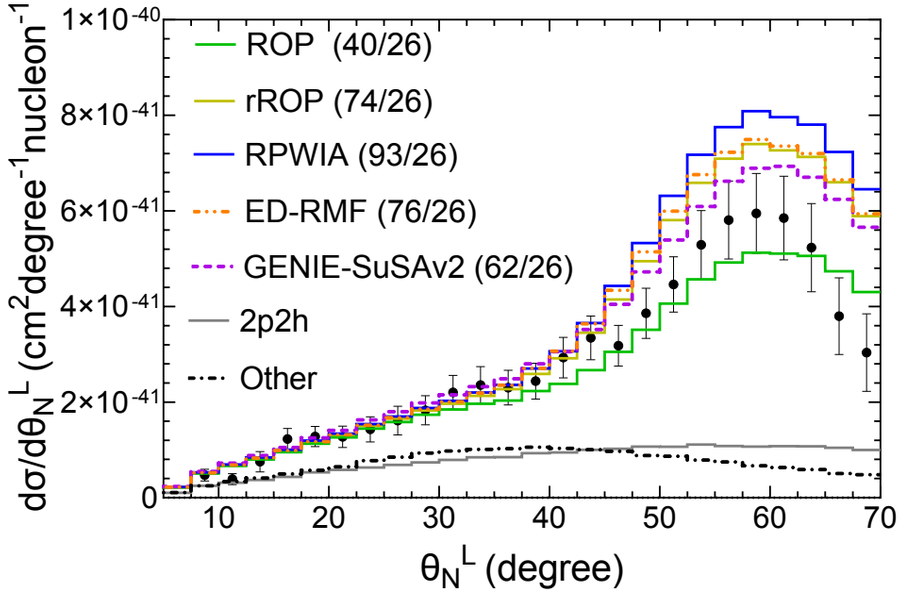

- ROP is favoured by data
- 2p2h provide ~30% of the strength at MINERvA kinematics (E ~ 3 GeV)

MINERvA

1μCC0πNp with at least one proton in the final state

TKI variables

kinematic restrictions

MINERνA	k' (GeV)	$\cos\theta_l$	p_N (GeV)	$\cos\theta_N^L$	ϕ_N^L (°)
	1.5-10	> 0.939	0.45-1.2	> 0.342	-

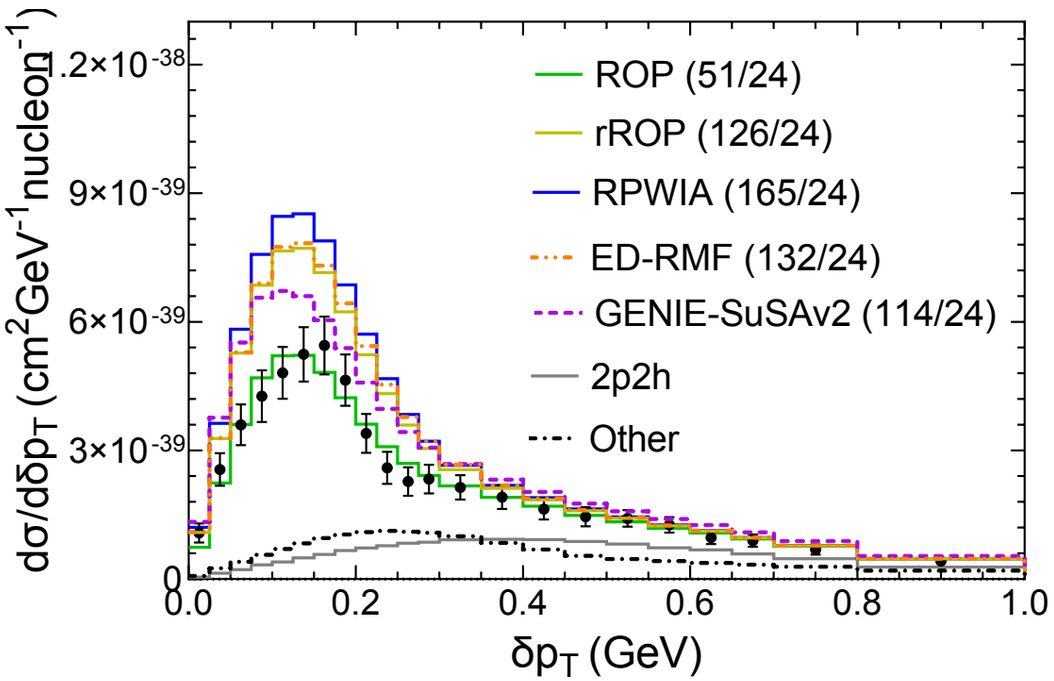

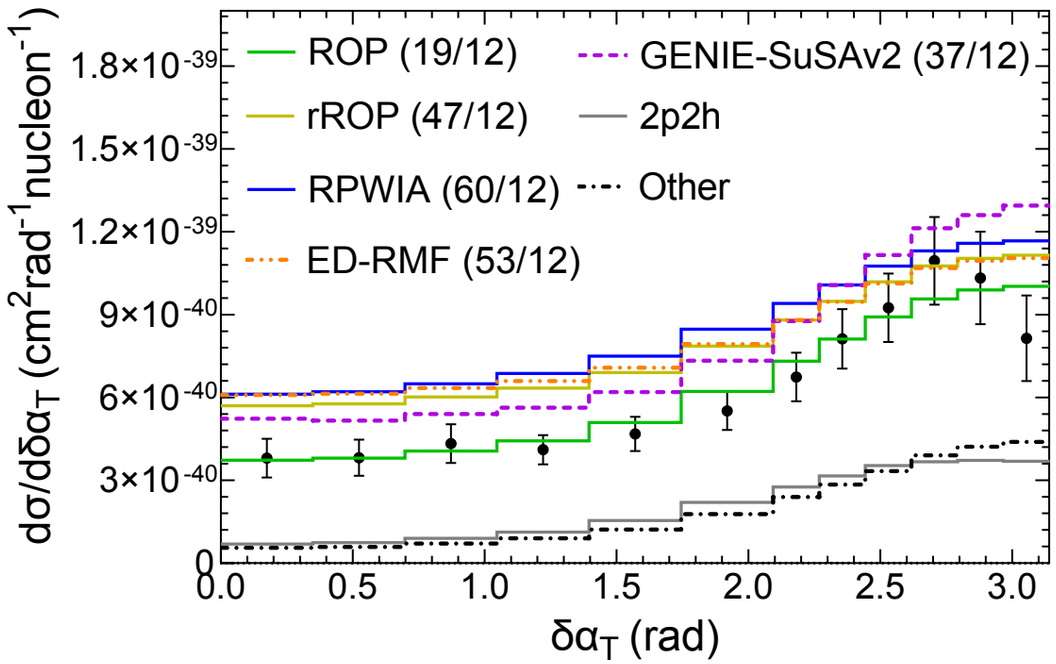

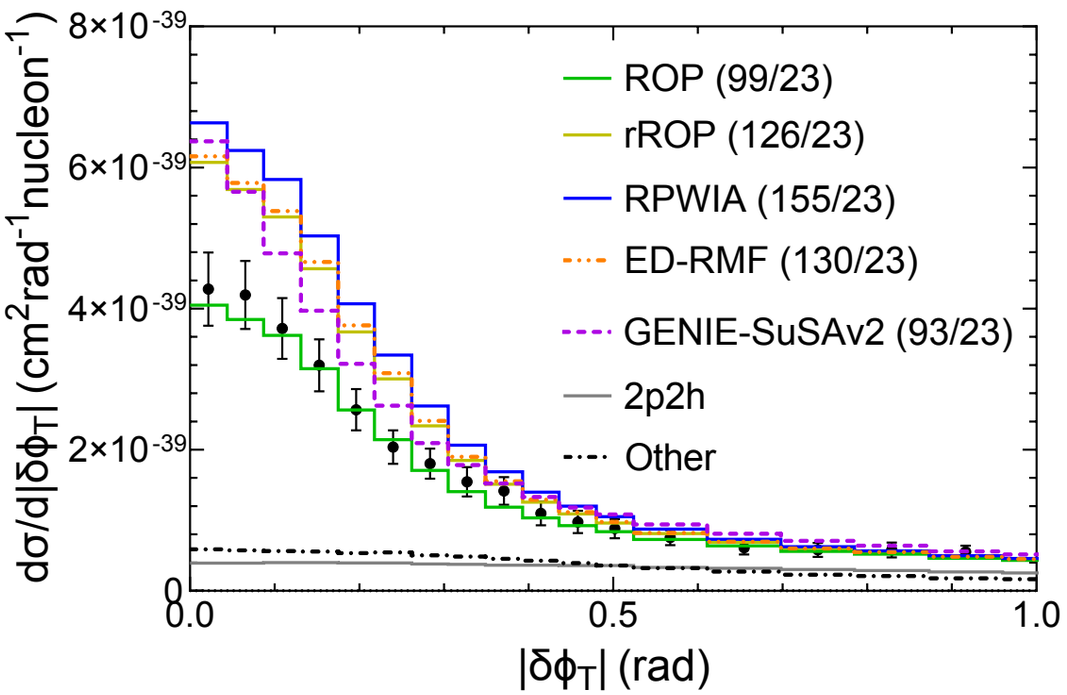

- ROP is favoured by data
- 2p2h provide ~30% of the strength at MINERvA kinematics (E ~ 3 GeV)

MicroBooNE

1μCC0πNp "at least one proton"

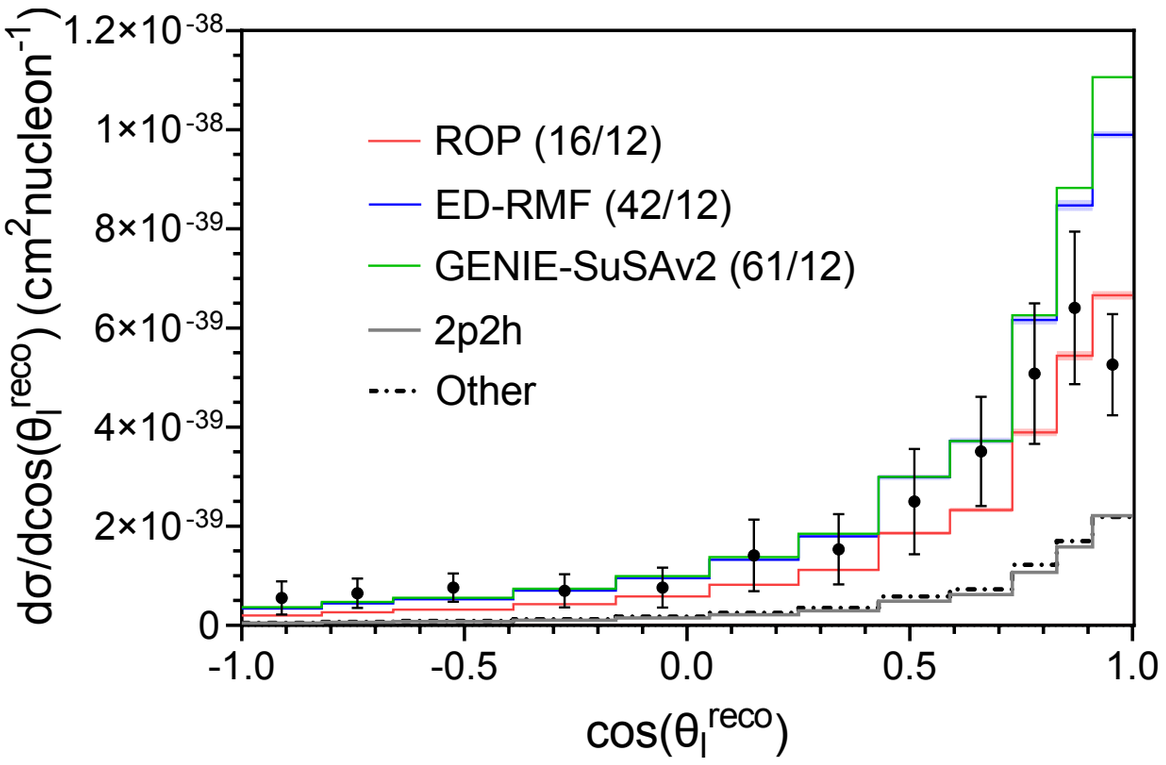

- ROP model is the closest to data
- 2p2h give sizeable contribution and are evaluated using GENIE simulation, based on inclusive SuSAv2-MEC model
- Microscopic calculations for exclusive 2p2h are much needed!

1μCC0π1p "one and only one proton"

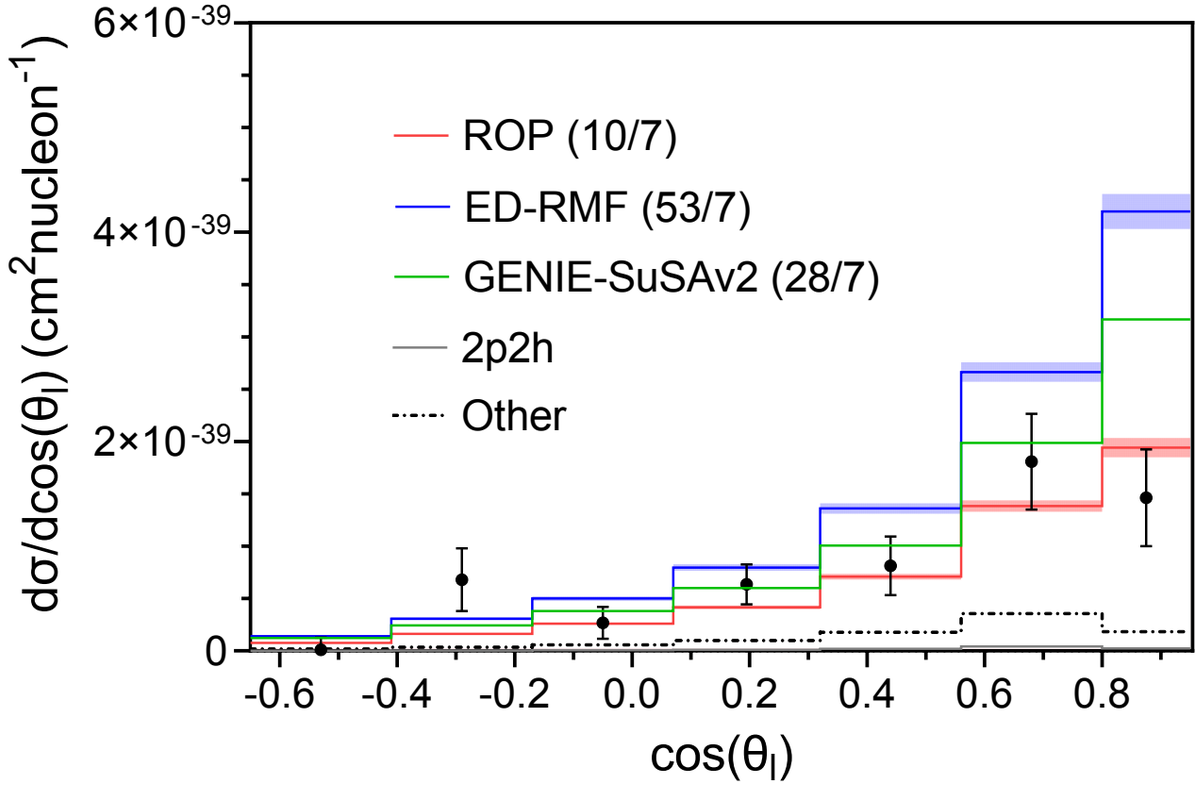

- ROP model is the closest to data
- 2p2h are negligible in the "only one proton" data

Inelastic region

Modelling the inelastic region will be essential for the future DUNE experiment

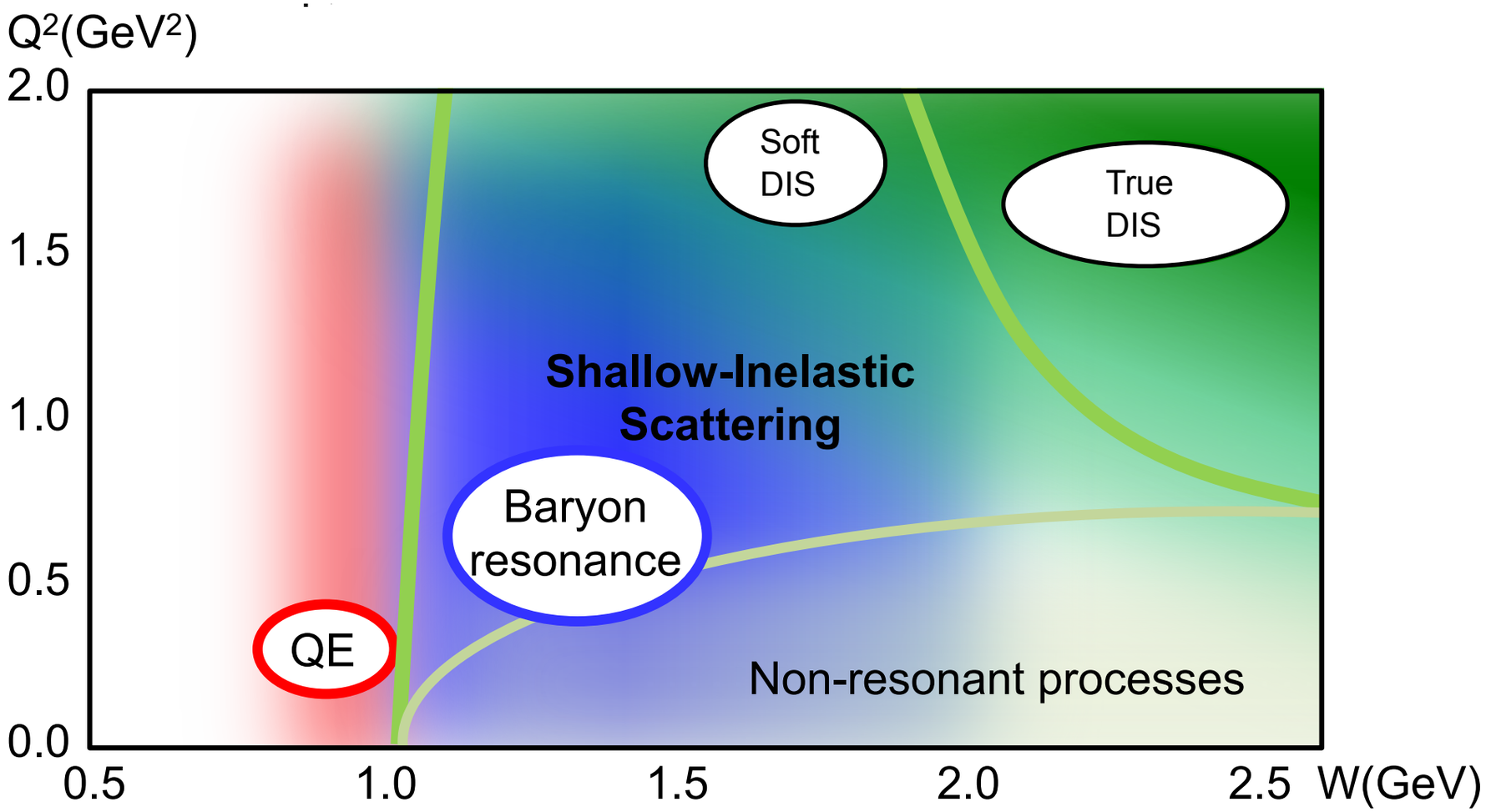

Inelastic response functions

$$R^K_{inel}(q,\omega) \propto \int_{W_{min}}^{W_{max}} dW_X f(\psi_X)\, U^K_{inel}(q,\omega)$$

SuSAv2

Process	Region	Model
RES	W < 2.1 GeV	DCC model Osaka group
TrueDIS	W > 2.1 GeV	PDF
SoftDIS	overlap between TrueDIS and RES region tuned by kinematic cuts	

details in J. Gonzalez-Rosa et al., arXiv:2306.12060 [nucl-th]

Resonance region: SuSAv2-DCC model

To describe the inelastic $\nu - N$ scattering in the RES region we use the **Dynamical Coupled Channel** model [S. Nakamura et al., PRD 92 (2015)]

- Widely tested for electron and neutrino scattering off a single nucleon
- Describes the resonant and non-resonant regimes, including the interaction between the different resonance channels (πN, $\pi\pi$N, ηN, KΛ, KΣ), the interference between resonant and non-resonant amplitudes and the neutrino induced two-pion production.
- Validity range $m_N + m_\pi < W < 2.1\,\text{GeV}$

$e - p$

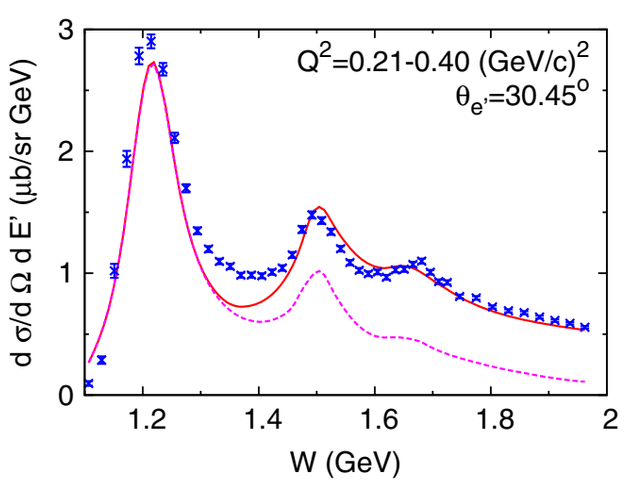

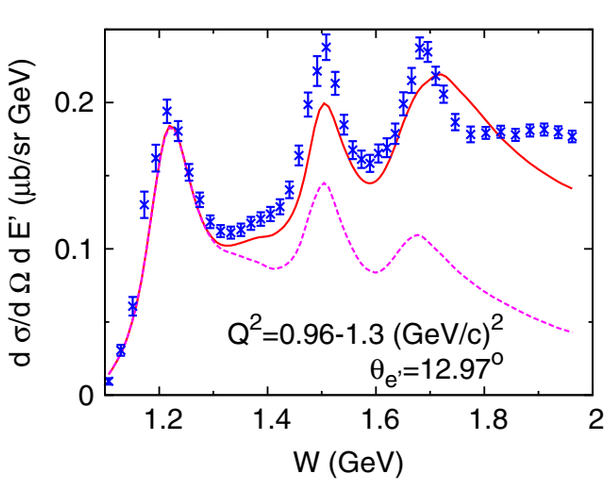

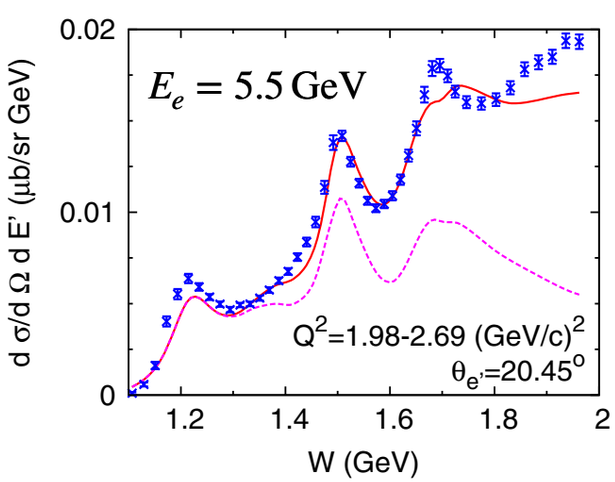

$\nu - N$

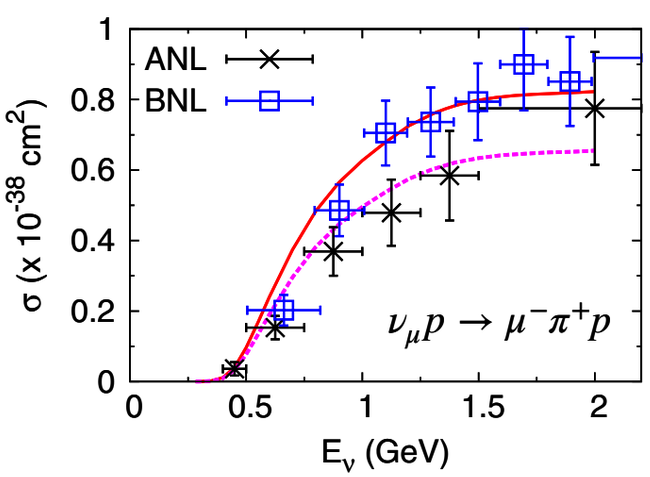

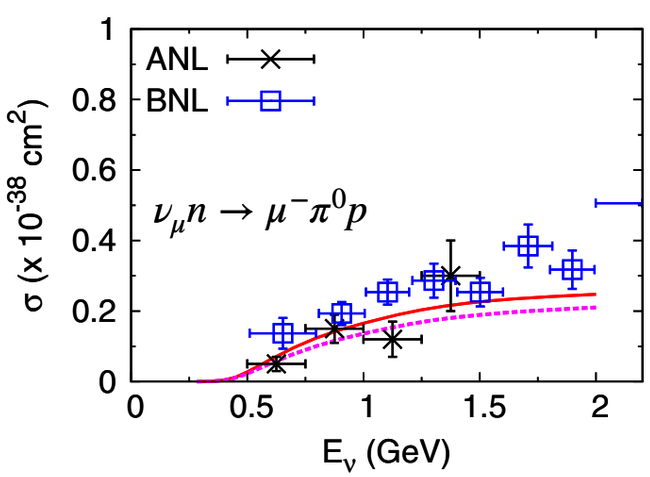

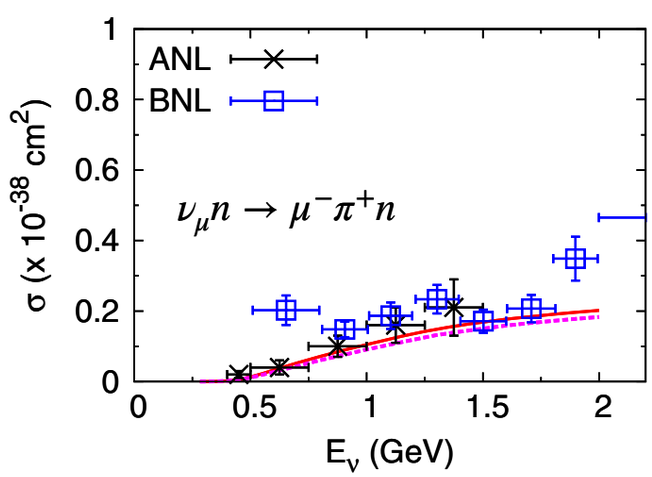

Validation: electron scattering

$e - {}^{12}C$

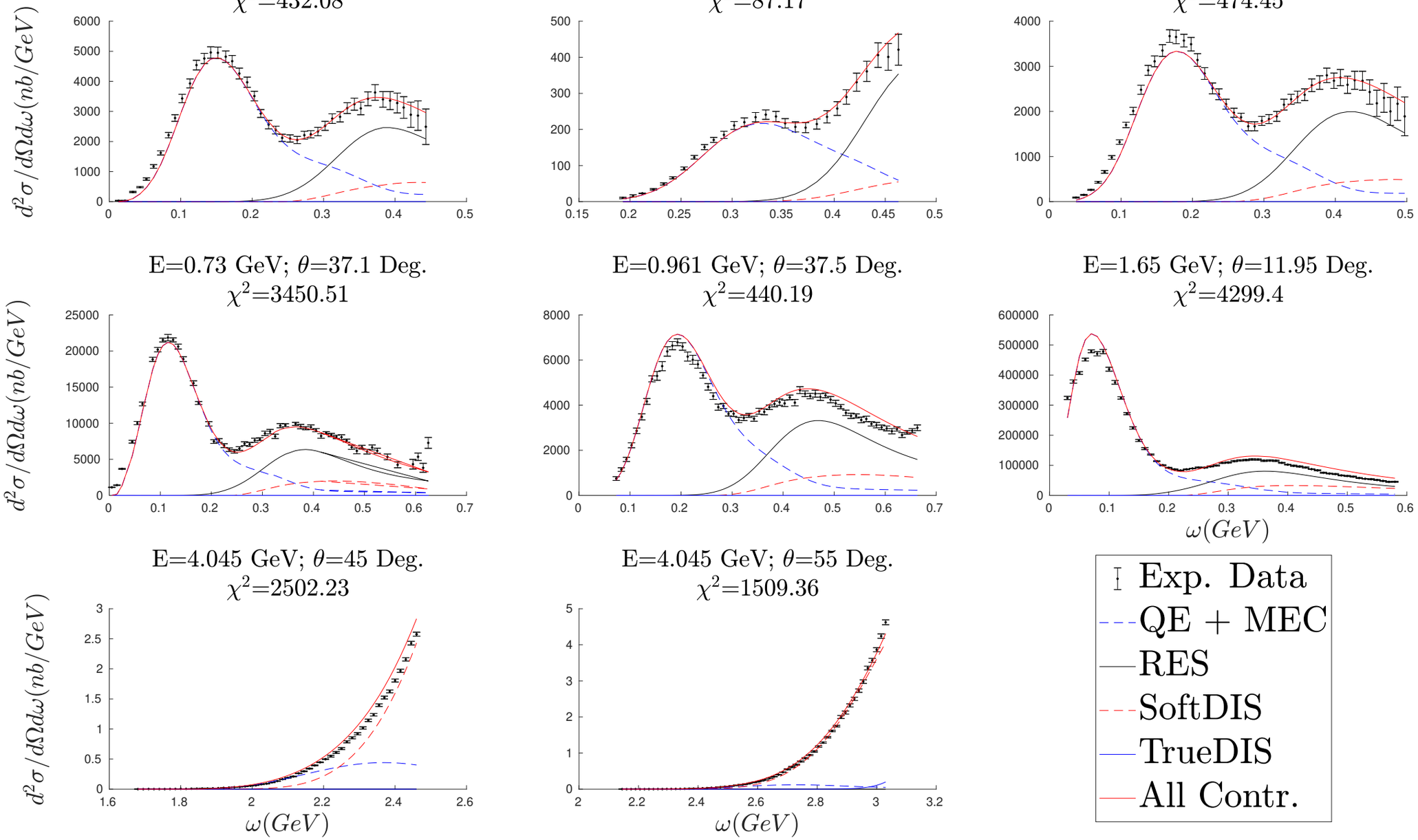

J. Gonzalez-Rosa et al., arXiv:2306.12060 [nucl-th]

Inclusive neutrino scattering in the SuSAv2-DCC model

T2K E ~ 0.6 GeV

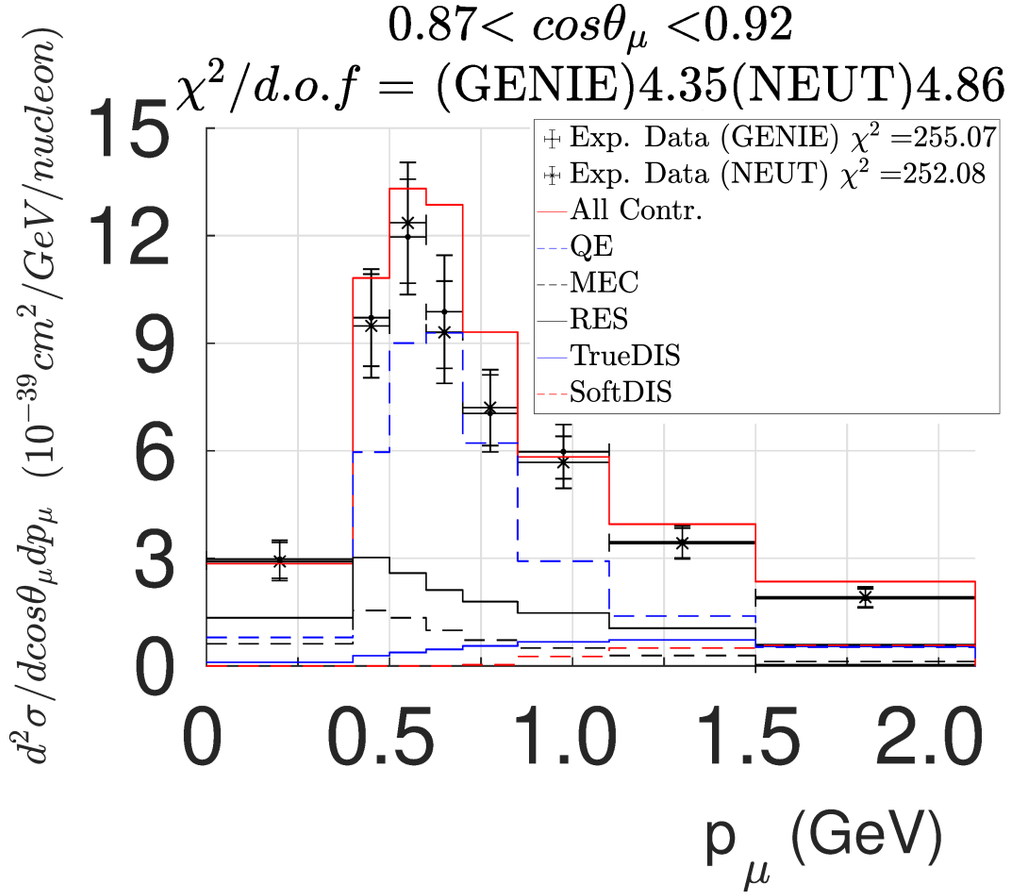

- Fair agreement with data
- QE dominates
- RES essential to reproduce the data
- DIS small contribution

MINERvA (ME) E ~ 6 GeV

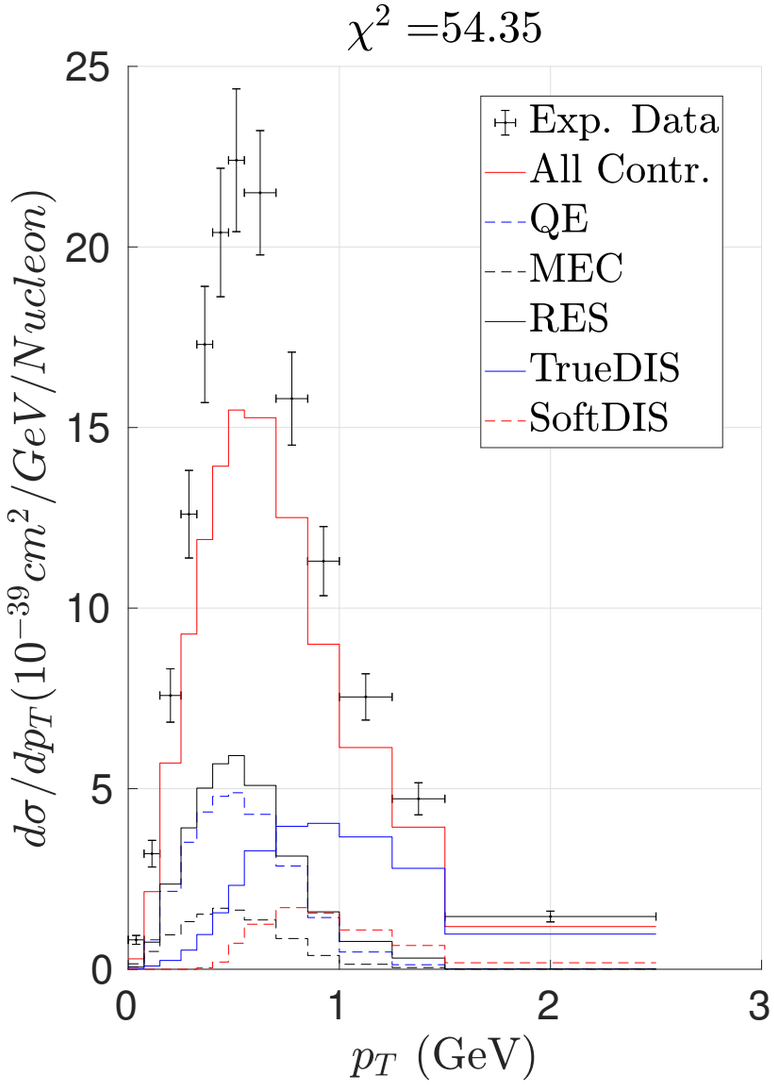

- Data are underestimated
- All channels are comparable in size
- The discrepancy is likely due to poor description of the “SoftDIS” region

J. Gonzalez-Rosa et al., arXiv:2306.12060 [nucl-th]

Summary

- The consistent microscopic description of neutrino scattering in different energy regimes, going from QE to DIS, is crucial for future oscillation experiments but quite hard to achieve. The present situation does not match the desired precision.

- The SuSAv2 model with the addition of 2p2h has been successfully tested against inclusive (e,e') data and used to evaluate CC0π neutrino cross sections as functions of the lepton variables, yielding results compatible with errorbars.

- Experimental studies (T2K, MINERvA, MicroBooNE) are moving in the direction of semi-inclusive measurements, where both leptons and hadrons are detected in the final state. These data are far more sensitive to nuclear effects and theoretical studies are very rare. We have studied this process in the framework of RMF and compared results with available data.

- In particular the sensitivity to different treatments of FSI has been explored and the ROP seems to be favoured by data. However, the results strongly depend on the contribution of two-body currents to the semi-inclusive process, which at present are simulated by Monte Carlo generators under strong assumptions since a microscopic calculation is still missing.

WORK IN PROGRESS

1. calculation of the 2p2h contribution to exclusive observables
2. comparisons and improvement of models for the low energy part of the spectrum, where the IA fails

   (see Valerio Belocchi's talk)

3. improvement of the model for the high energy spectrum, from the resonance region to DIS; this region will be essential for DUNE.

Backup slides

Scaling variable

The scaling variable ψ is defined in the framework of QE scattering the relativistic Fermi gas model

$$\psi(q,\omega) \equiv \pm\sqrt{\frac{T_0}{T_F}} \qquad T_0 = \frac{q}{2}\sqrt{1+1/\tau} - \frac{\omega}{2} - m_N$$

T_0 is the minimum kinetic energy of the hit nucleus at given momentum and energy transfer

$$\psi(q,\omega) \simeq \frac{m_N}{qk_F}\left(\omega - \frac{|Q^2|}{2m_N}\right)$$

$\psi = 0$ at the QEP

In the relativistic Fermi gas model

$$f^{RFG}(\psi) = \frac{3}{4}\left(1-\psi^2\right)\theta\left(1-\psi^2\right)$$

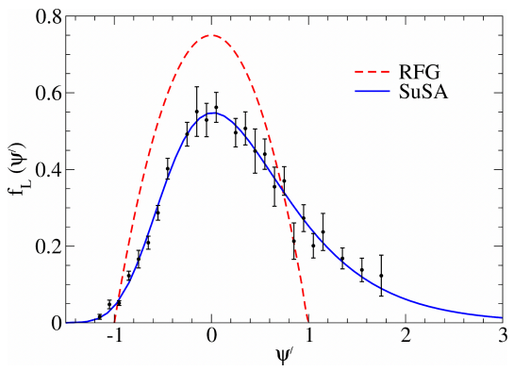

ψ is analogous to the Bjorken variable x in DIS

Extension to the inelastic regime

$$\psi(q,\omega) \equiv \pm\sqrt{\frac{T_0^*}{T_F}}$$

$$T_0^* = \frac{q}{2}\sqrt{1+1/\tau} - \frac{\omega}{2} - W$$

W is the invariant mass of the final hadronic state

Super Scaling in the Longitudinal and Transverse channels

Donnelly and Sick, PRL82; PRC60 (1999)

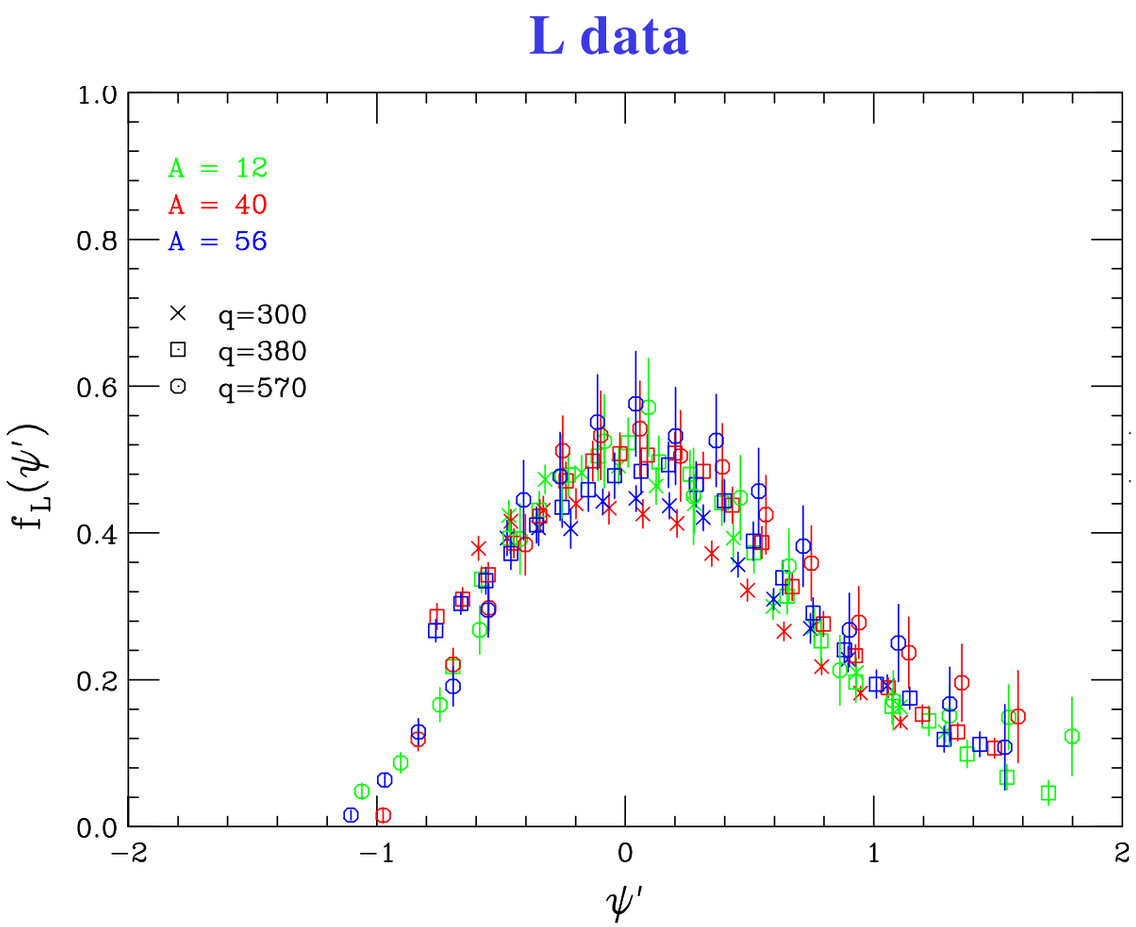

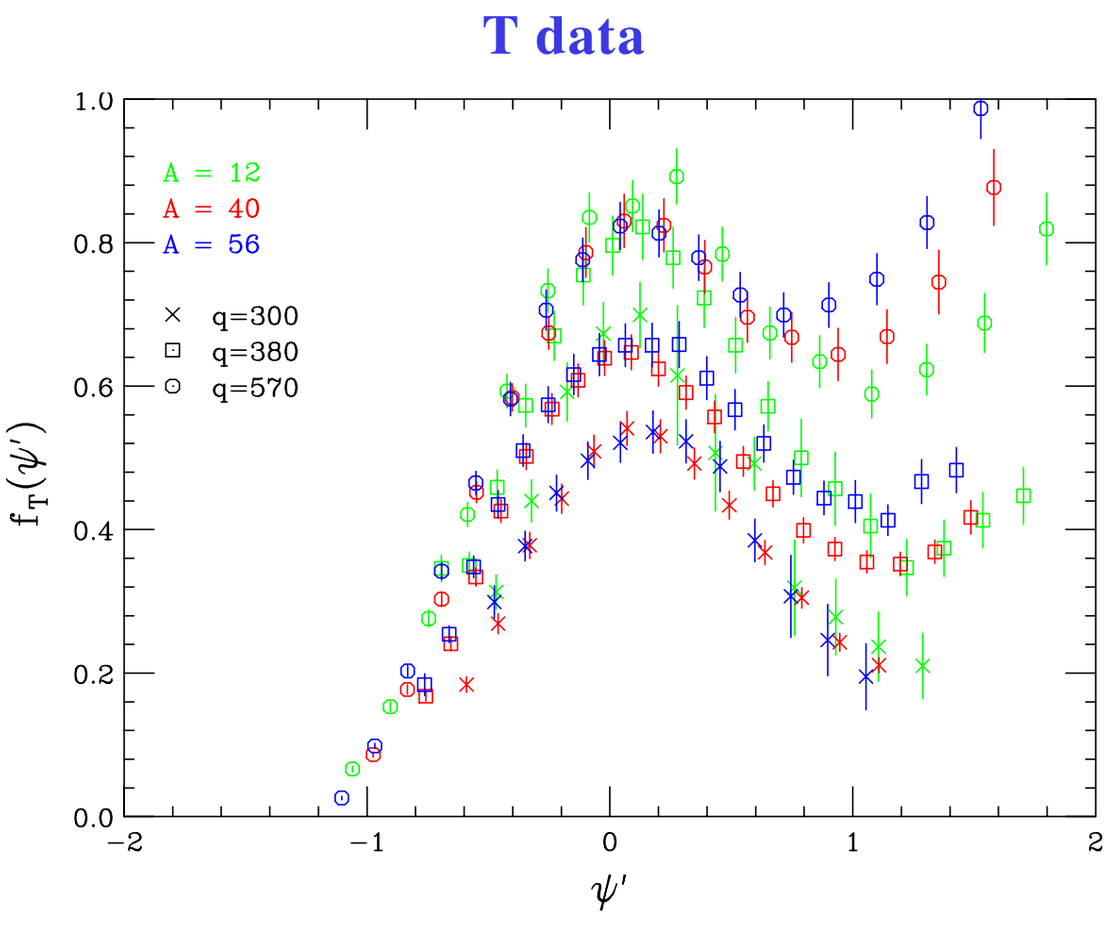

The analysis of the separate longitudinal and transverse responses shows that

- the **longitudinal response scales**

- **scaling violations** are mainly **transverse** (2p2h, Δ resonance and other inelastic processes)

MEC in the 1p1h channel

Two-body currents can also excite 1p1h states

$$W^{\mu\nu}_{1p1h} \sim \sum_{ph} < ph|\hat{J}^{\mu}|A >^{*} < ph|\hat{J}^{\nu}|A >$$

$$\hat{J}^{\mu} = \hat{J}^{\mu}_{1b} + \hat{J}^{\mu}_{2b} \rightarrow W^{\mu\nu}_{1p1h} = W^{\mu\nu}_{OB} + W^{\mu\nu}_{MEC} + W^{\mu\nu}_{OB-MEC}$$

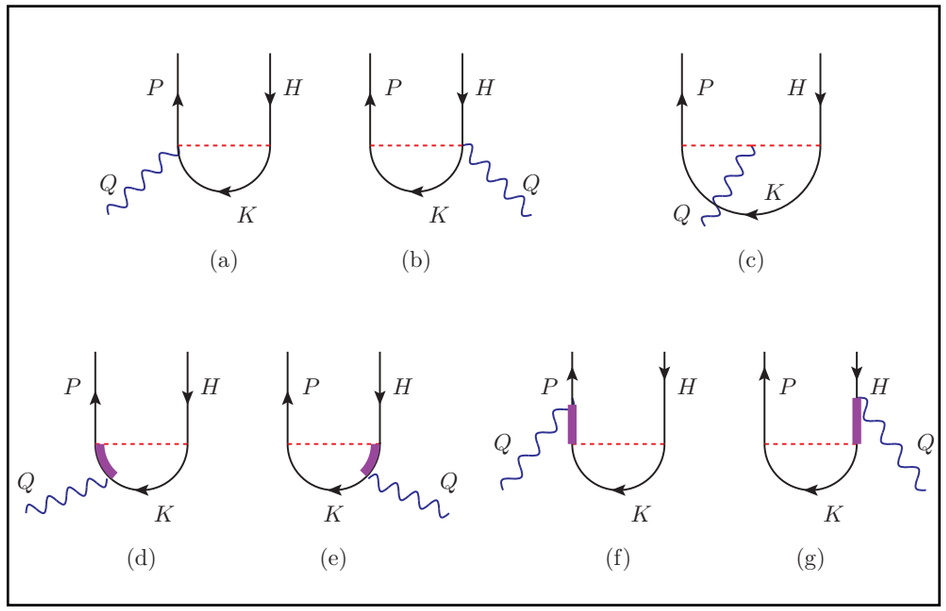

The negative interference dominates

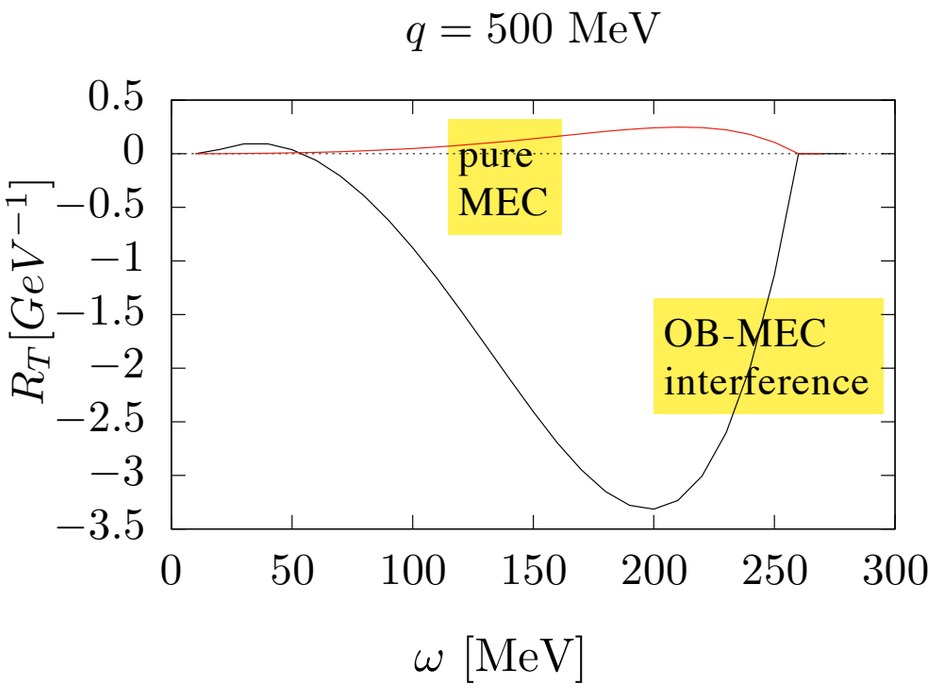

1p1h MEC can be incorporated in the SuSA formalism

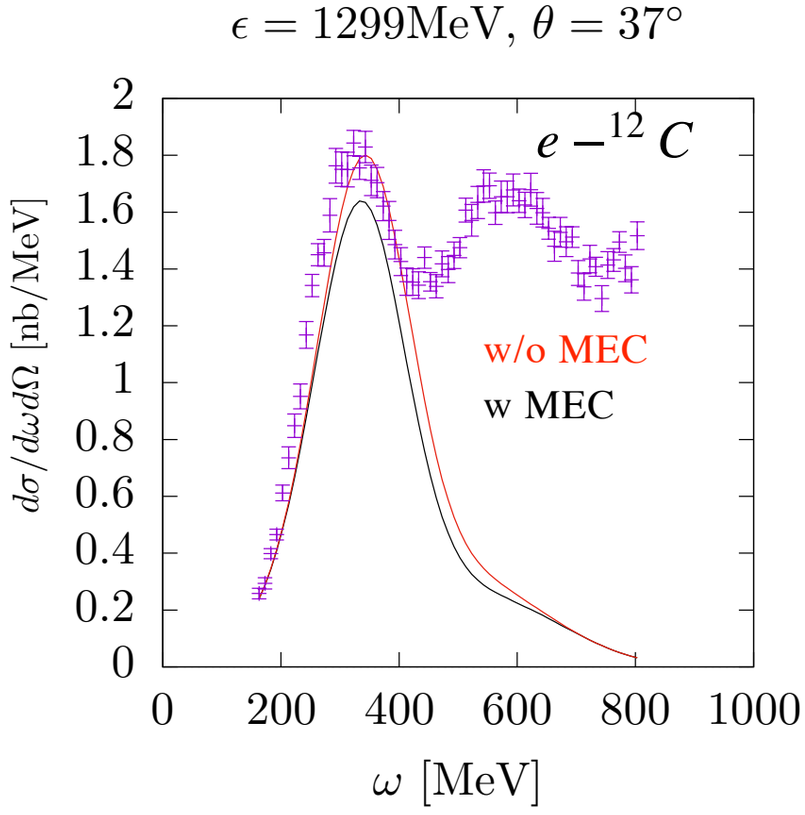

P. Casale, J.E. Amaro, MBB, arXiv:2307.15783 [nucl-th]

Neutral Current neutrino scattering and the nucleon's strangeness

Collaboration with Carlotta Giusti, Martin Ivanov and Stephen Pate

Neutral current (anti)neutrino-nucleus cross section gives access to the strange form factors of the nucleon

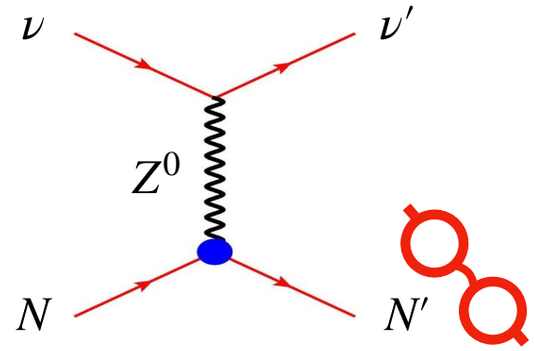

$$\frac{d\sigma}{dE_N d\Omega_N} \sim l_{\mu\nu} W^{\mu\nu} = x_0 \left[v_L R_L + v_T R_T + v_{TT} R_{TT} + v_{TL} R_{TL} \pm \left(2 v_{T'} R_{T'} + 2 v_{TL'} R_{TL'} \right) \right]$$

$$\begin{aligned}
R_L &= -w_1(\tau)\frac{\kappa^2}{\tau} + w_2(\tau)(\varepsilon+\lambda)^2 \\
R_T &= 2w_1(\tau) + w_2(\tau)\eta^2 \sin^2\theta \\
R_{TT} &= -w_2(\tau)\eta^2 \sin^2\theta \cos(2\phi) \\
R_{TL} &= 2\sqrt{2} w_2(\tau)(\varepsilon+\lambda)\eta \sin\theta \cos\phi \\
R_{T'} &= 2w_3(\tau)\frac{\tau}{\kappa}(\varepsilon+\lambda) \\
R_{TL'} &= 2\sqrt{2} w_3(\tau)\kappa\eta \sin\theta \cos\phi
\end{aligned}$$

$$\begin{aligned}
w_{1a}(\tau) &= \tau \widetilde{G}^2_{Ma}(\tau) + (1+\tau)\widetilde{G}^2_{Aa}(\tau) \\
w_{2a}(\tau) &= \frac{\widetilde{G}^2_{Ea}(\tau) + \tau \widetilde{G}^2_{Ma}(\tau)}{1+\tau} + \widetilde{G}^2_{Aa}(\tau) \\
w_{3a}(\tau) &= \widetilde{G}_{Ma}(\tau)\widetilde{G}_{Aa}(\tau)
\end{aligned}$$

$$\begin{aligned}
\widetilde{G}_{Ep}(\tau) &= (2 - 4\sin^2\theta_W) G_E^{T=1}(\tau) \\
&\quad - 4\sin^2\theta_W G_E^{T=0}(\tau) - G_E^{(s)}(\tau) \\
\widetilde{G}_{En}(\tau) &= -(2 - 4\sin^2\theta_W) G_E^{T=1}(\tau) \\
&\quad - 4\sin^2\theta_W G_E^{T=0}(\tau) - G_E^{(s)}(\tau) \\
\widetilde{G}_{Mp}(\tau) &= (2 - 4\sin^2\theta_W) G_M^{T=1}(\tau) \\
&\quad - 4\sin^2\theta_W G_M^{T=0}(\tau) - G_M^{(s)}(\tau) \\
\widetilde{G}_{Mn}(\tau) &= -(2 - 4\sin^2\theta_W) G_M^{T=1}(\tau) \\
&\quad - 4\sin^2\theta_W G_M^{T=0}(\tau) - G_M^{(s)}(\tau) \\
\widetilde{G}_{Ap}(\tau) &= -2G_A^{(3)}(\tau) + G_A^{(s)}(\tau) \\
\widetilde{G}_{An}(\tau) &= 2G_A^{(3)}(\tau) + G_A^{(s)}(\tau).
\end{aligned}$$

Complementary information on strange FFs from PVES with polarised electrons $\vec{e}p$, $\vec{e}d$ and $\vec{e}\,^4He$

✦ Previous simultaneous determination of $G_E^s(Q^2)$, $G_M^s(Q^2)$ and $G_A^s(Q^2)$ from PVES and NCE $\nu(\bar{\nu})$-N data

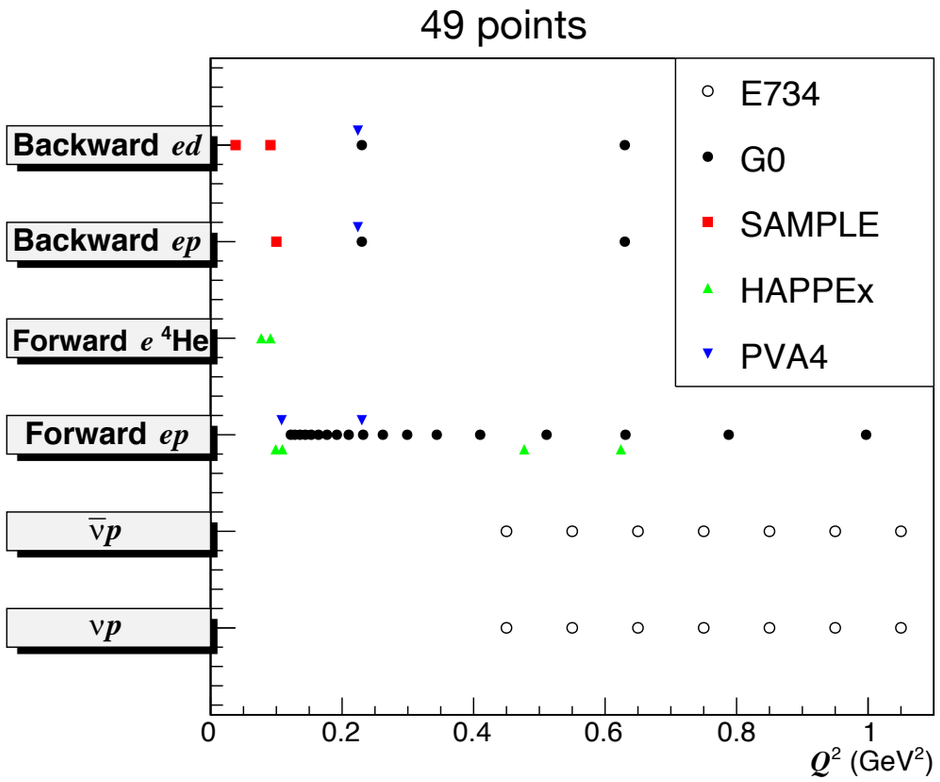

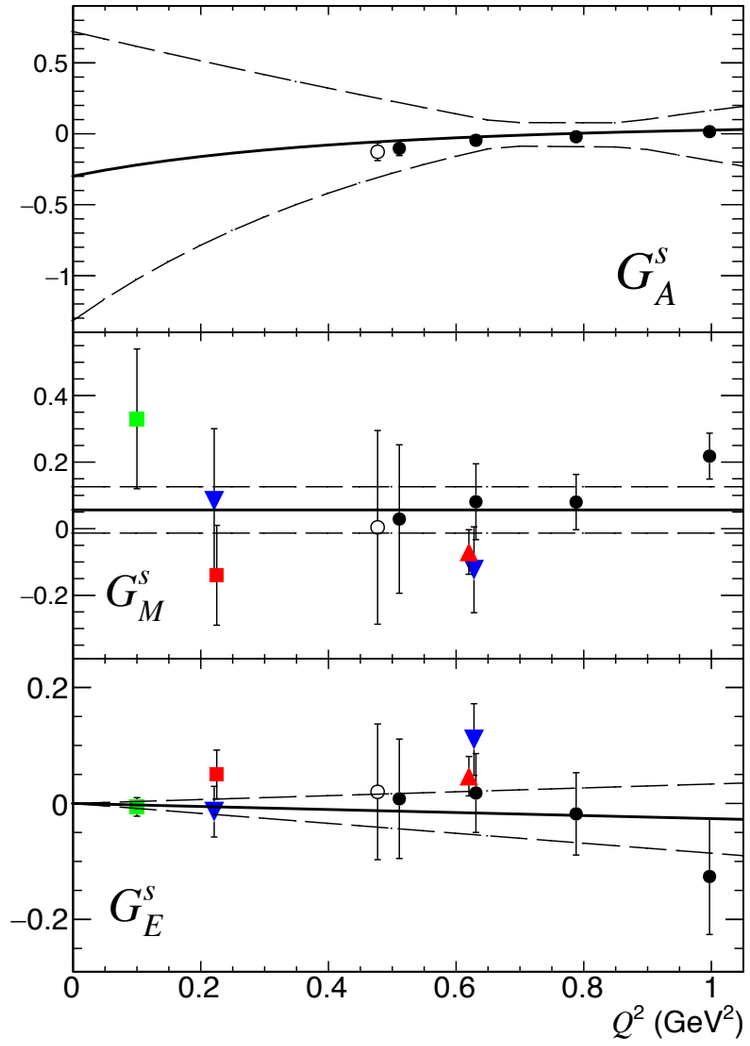

- G0 (forward *ep*) + E734 (*νp* and $\bar{\nu}p$)
- HAPPEx (forward *ep*) + E734 (*νp* and $\bar{\nu}p$)
  Pate, Papavassiliou & McKee, PRC 78 (2008) 015207

- PVA4 (forward and backward *ep*)
  Baunack et al., PRL 102 (2009) 151803

- G0 (forward and backward *ep*, and backward *ed*)
  D. Androic et al., PRL 104 (2010) 012001

- HAPPEx (forward *ep* and e^4He) + G0 (forward *ep*)
  + SAMPLE (backward *ep* and *ed*) + PVA4 (forward *ep*)
  near $Q^2 = 0.1$ GeV^2
  Liu, McKeown & Ramsey-Musolf, PRC 76 (2007) 025202

- HAPPEx (forward *ep*) + G0 (forward and backward *ep*)
  Ahmed et al. PRL 108 (2012) 102001

➡ Good determination of the s-quark contribution to the **vector** form factors (consistent with zero)

➡ **Poor determination of the axial form factor** due to lack of NCE data at low Q^2

➡ **Including MiniBooNE and (future) MicroBooNE** data in the fit will improve the knowledge of G_A^s

➡ **Nuclear models** are needed for CH_2 (MB) and *Ar* (μB)

Model comparison with MiniBooNE data

M. Ivanov et al., *Phys.Rev.C* 91 (2015)

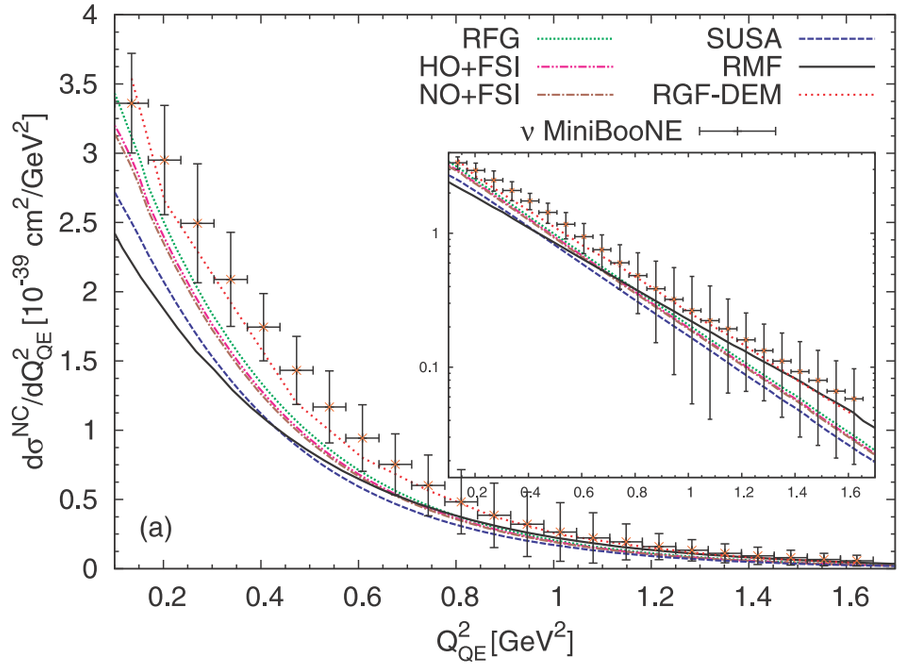

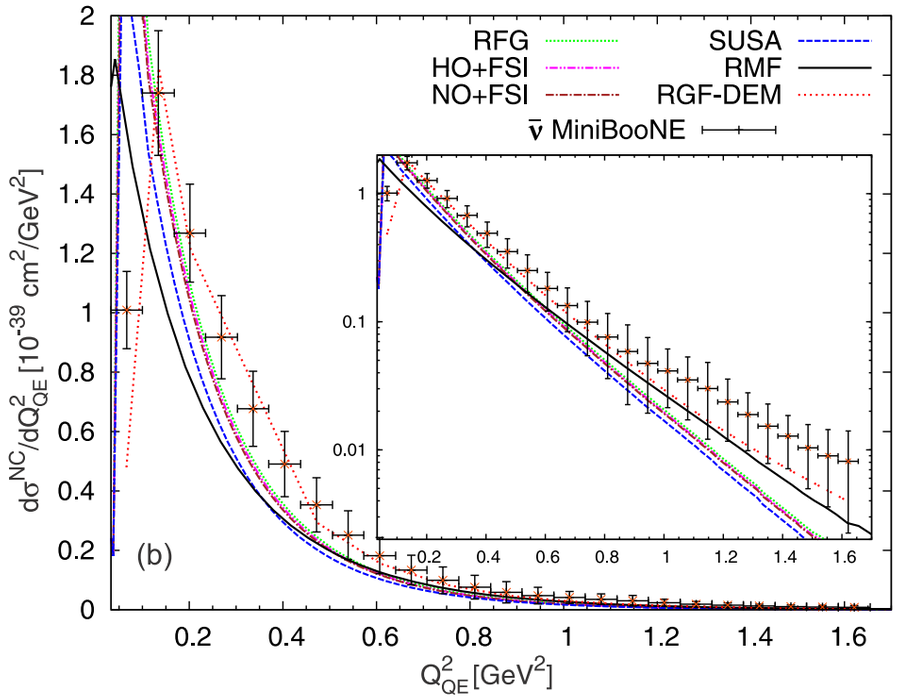

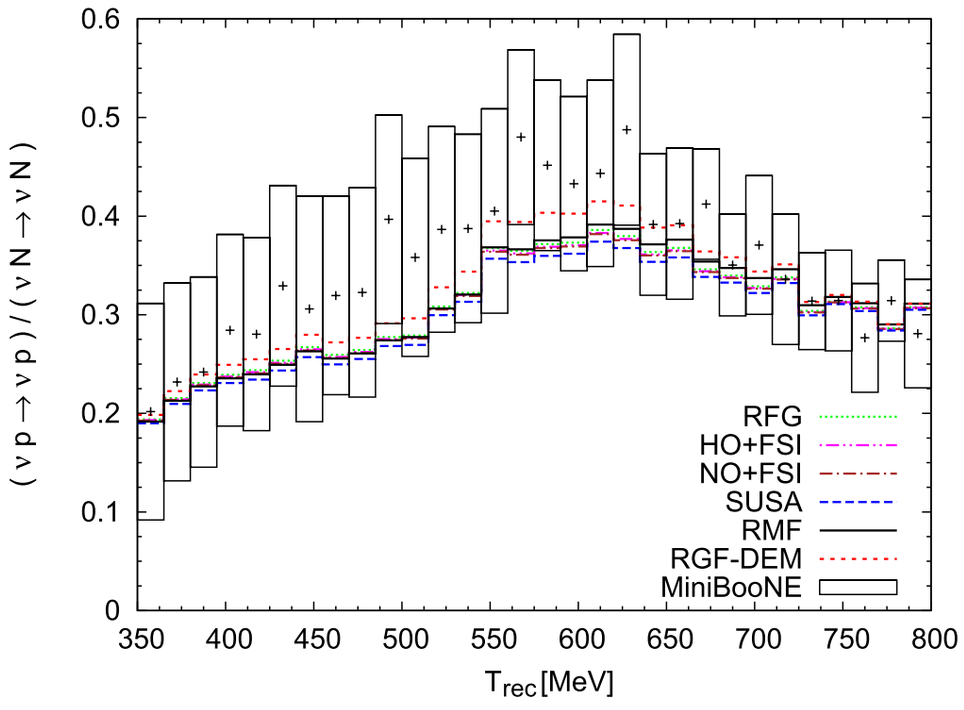

➡HO and NO are two versions of the Spectral Function SF model

➡ **Differences between models are non-negligible in cross sections but very small in the p/N ratio**

➡ The Relativistic Green Function model RGF-DEM and the RMF are too time-consuming for this kind of analysis → we limited the study to SuSA and SF models

Preliminary results

Without MiniBooNE

With MiniBooNE

SuSA

SF

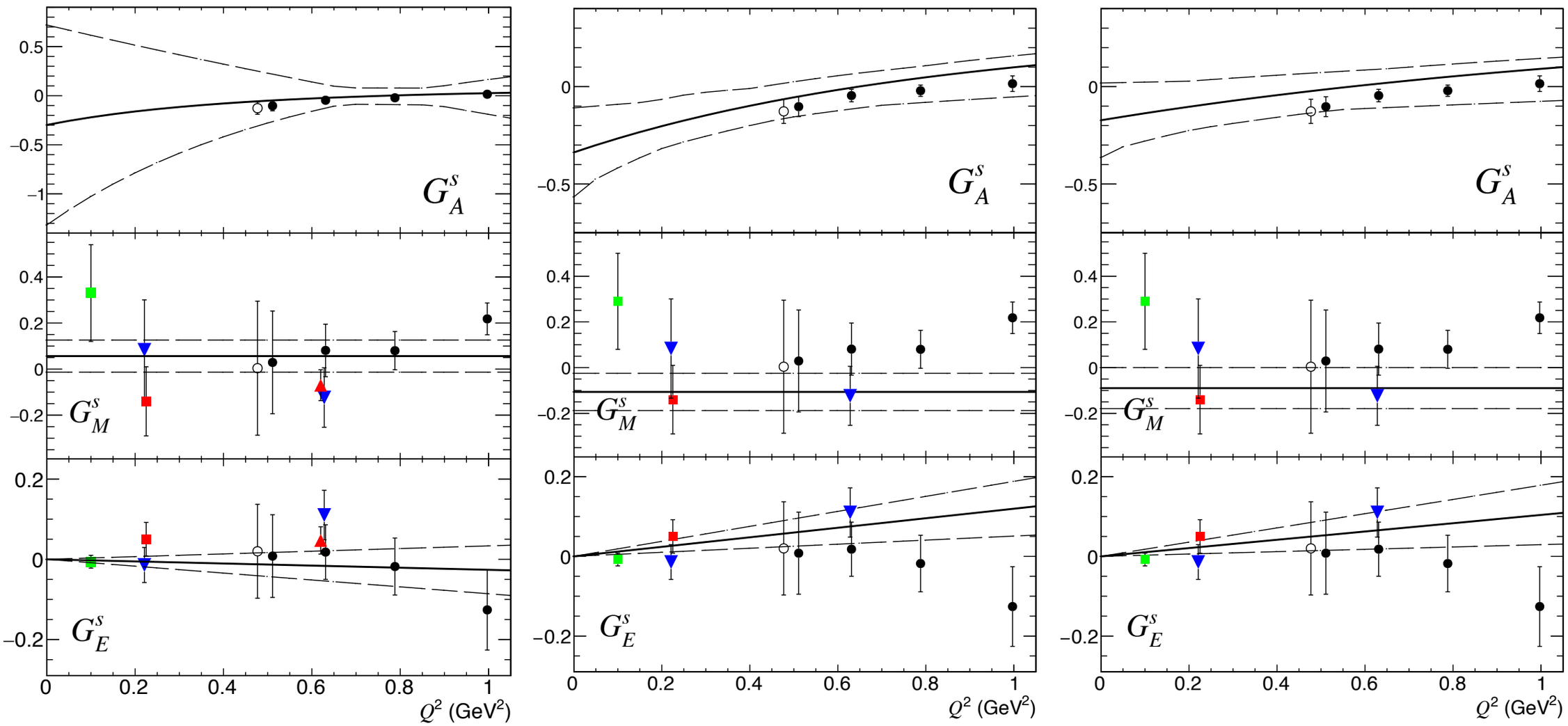

✓ **Great improvement of limits on G_A^s**

The low Q^2 region will be filled by future MicroBooNE data (more statistics, Q^2 down to 0.1 GeV^2)